

CHAPTER 1

**Design and Syntheses of Palladium
Complexes of NNN/CNN Pincer Ligands:
Catalyst for Cross-Dehydrogenative
Coupling Reaction of Heteroarenes**

1.1 INTRODUCTION

Bi(hetero)aryl is a basic skeleton of the organic compounds, which has been found in many natural products, polymers, advanced materials, ligands, pharmaceuticals and medicinal chemistry.¹⁻² Moreover, bi(hetero)aryl act as a chromophore, found in numerous drugs such as antifungal, anticancer, antibiotics and anti-hypertensive agents. In the assessment of bi(hetero)aryls, organic chemists have made extensive efforts for the development of more effective and straightforward methodologies for the formation of bi(hetero)aryl carbon-carbon bond with excellent selectivity under mild reaction conditions.³ Despite the many advantages of these traditional methods, some of the significant challenges are also found. As a result, scientific community has discovered the new era of transition metal-catalyzed reactions for the construction of carbon-carbon bond. The newly developed transition metal-catalyzed strategy provides the straightforward and an efficient way to access the bi(hetero)cyclic compounds.⁴⁻⁵

1.1.1 Transition Metal-Catalyzed Reaction

During past five decades, transition metal-catalyzed coupling reactions played a remarkable role in the construction of bi(hetero)cyclic compounds because of their extended scope and practicability. Due to the easy access of these transformations, it is exclusively studied in academic level as well as chemical industries and various synthetic technologies.⁶ In 2010, the Nobel prize in Chemistry was awarded to Suzuki, Mizoroki–Heck, Negishi for their exertions in organic synthesis towards palladium-catalyzed cross-coupling reactions.⁷⁻⁹ The transition metal-catalyzed cross coupling between (hetero)aryl halide or triflate with organometallic reagents, such as the Suzuki and Negishi reactions, delivered the efficient protocol for the construction of bi(hetero)aryl compounds (**Figure 1.1**).¹⁰ These are the most reliable methods to provides a high yield of cross-coupled heteroaromatic products with predictable regioselectivity. However, these methods suffer some limitations to make it non-ideal. In view of substrates, utilization of prefuntionalized starting materials like heteroaryl organometallic reagents and pseudohalides are not readily accessible and may also ineffectively contribute to the coupling reaction. Moreover, heteroaryl-heteroaryl bond formation is irregular, because of the reactivity and selectivity of coupling partners in the coupling reaction. From green chemistry perspective, the poor atom economy made this methodology non-ideal and non-sustainable for the synthesis of bi(hetero)aryls.¹¹ As a result, the replacement of

traditional methods with another effective approach is highly appealing, which help to overcome these limitations to some extent.

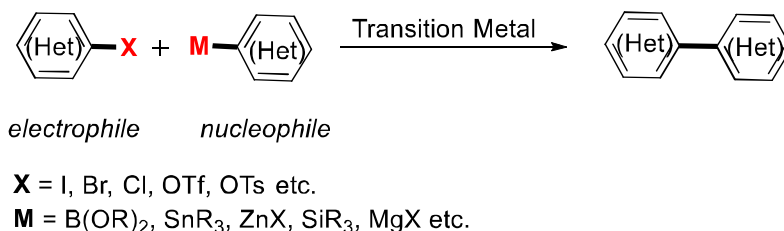


Figure 1.1 Traditional transition metal-catalyzed cross-coupling reactions

1.1.2 Transition Metal-Catalyzed C–H Bond Activation

From the viewpoints of high efficiency and step economy, the synthesis of bis(hetero)aryl compounds through transition metal-catalyzed C–H bond activation of unactivated heteroarenes is an eco-friendly, attractive, and economic alternative approach.¹²⁻¹³ In recent years transition metal-catalyzed functionalization of organic compounds involving C–H activation pathway has been exclusively explored (**Figure 1.2**).¹⁴

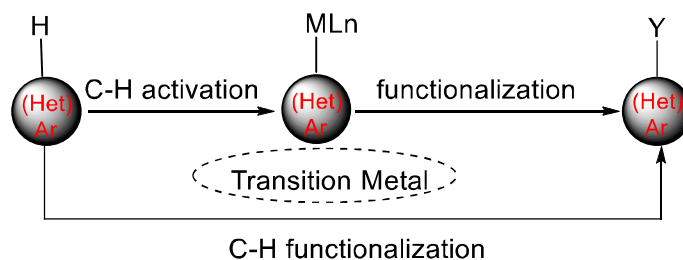
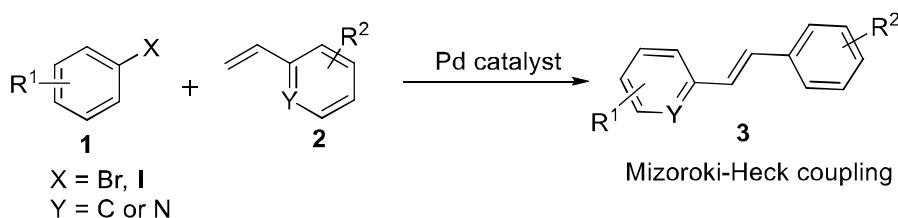


Figure 1.2 Transition metal-catalyzed C–H functionalization

The first report of C–H activation was described by Mizoroki-Heck in 2010.¹⁵ This reaction provides an inevitable tool for the synthesis of unsaturated alkenes using heteroaryl halides with substituted alkenes (**Scheme 1.1**). The requirement of only one preactivated coupling partner is the major advantage of this methodology.



Scheme 1.1 Mizoroki-Heck coupling reactions

However, it suffers some disadvantages *viz.* preinstallation of directing groups and activating the inert C–H bond as well as the selective functionalization of a single C–H bond within a whole molecule. Therefore, the heteroaryl-heteroaryl C–C bond formation would be ideal by the replacement of C–X or C–M bond with C–H bond (**Figure 1.3**).

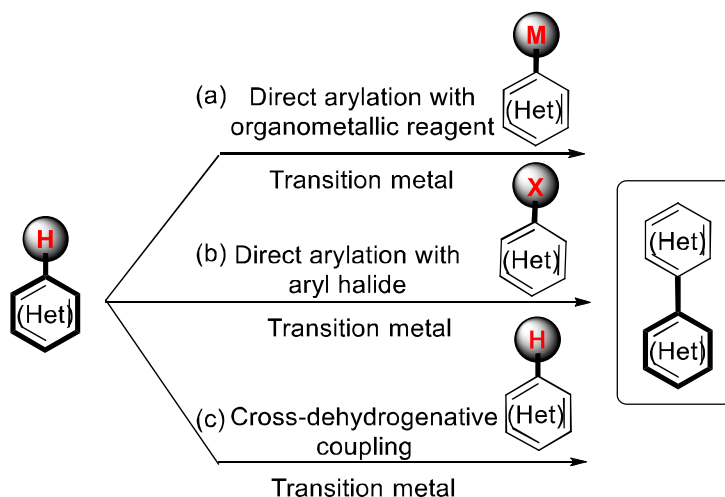


Figure 1.3 Transition metal-catalyzed C–H functionalization with different coupling partners

1.1.3 Transition Metal-Catalyzed Cross-Dehydrogenative Coupling Reactions

Owing to the importance of bi(hetero)aryl compounds, synthetic chemist always seeks to find out a more prominent route to access the C–C bonds.¹⁶ In recent years, the most direct approach for constructing carbon-carbon linkage from two simple carbon-hydrogen (C–H) bonds has emerged as an attractive and challenging goal in catalysis. In general, the coupling between two nucleophilic C–H bonds is termed as cross-dehydrogenative coupling (CDC) (**Figure 1.4**). These reactions required an external (or internal) oxidant to keep the process electroneutral. Because the evolution of H₂ gas is thermodynamically unfavorable and requires external driving force in the form of oxidant. Thus, this type of reaction is also called oxidative C–H/C–H coupling.¹⁷⁻¹⁹

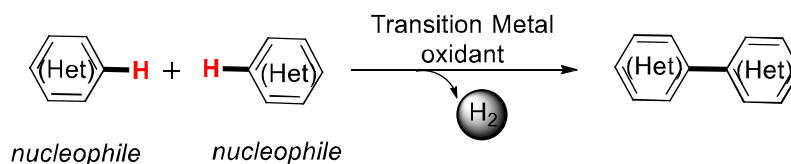


Figure 1.4 Transition metal-catalyzed oxidative coupling

The methodology has shown numerous advantages over the classical methods such as avoid prefunctionalization of substrate, reduces the number of steps for the synthesis of target molecules,²⁰⁻²¹ lower cost and lesser waste generation, step and atom economically favorable. The fast development of oxidative C–H/C–H coupling reactions between heteroarenes enables to forge bi(hetero)aryl linkage more concisely and economically. In order to these reactions are performed under aerobic conditions or with organic oxidants to provide an efficient and straightforward access to the π -conjugated poly(hetero)-aromatic compounds.²² Moreover, this type of reaction delivers a more convenient approach for the synthesis of natural products and the more susceptible for exploration of organic functional materials.

Despite many advantages, this concept encounters many major challenges as well. First, C–H activation required harsh reaction conditions because of aromatic C–H bond is an inert bond, which possesses higher bond dissociation energy than C–X and C–M bond.¹² Similarly, the regioselectivity concern of the C–H bond, the aromatic compounds typically contain multiple C–H bonds and it is highly challenging to activate a particular C–H bond.¹⁷ Likewise, site-selectivity issues, could be resolved by some strategies: first, switching and regulating the regioselectivity could be achieved by the selection of the catalytic system (catalytic system-based control). Second, effective use of the electronic nature of substrate, such as C–H activation occurs *via* the $S_{E}Ar$ pathway, metalation often takes place at the most nucleophilic position, whereas a CMD process occurs at the most acidic C–H bond.¹⁹ Third, incorporation of a directing group (chelation directed control). A Lewis basic heteroatom of the incorporated auxiliary group could coordinate to the catalyst and bring the metal close proximity to the specific C–H bond (usually *ortho* position) result to form five or six-membered metallocycle.²³ Fourth, the steric effect of substrate, due to steric hindrance some C–H bonds are more accessible to the catalyst.²⁴

In recent years, the synthetic organic community has given more attention towards oxidative cross-coupling methods because of the use of unactivated C–H precursors. Now it became not only a hot research topic but also a broad research area, due to its simplicity and applications in natural products, biologically important π -conjugated bi(hetero)aryl systems, and organic functional materials.²² As a result, several research groups published numerous review articles to summarize the transition metal-catalyzed oxidative cross-coupling reactions systematically up to 2016.^{12, 17, 19, 23-24} The classification of those reviews was described based on fundamental parameters such as, use of transition metal-catalyst frameworks, the pattern of coupling partners *i.e.* (hetero)arenes,

incorporation with or without directing groups, and nature of carbon atoms like sp , sp^2 , and sp^3 (Figure 1.5).

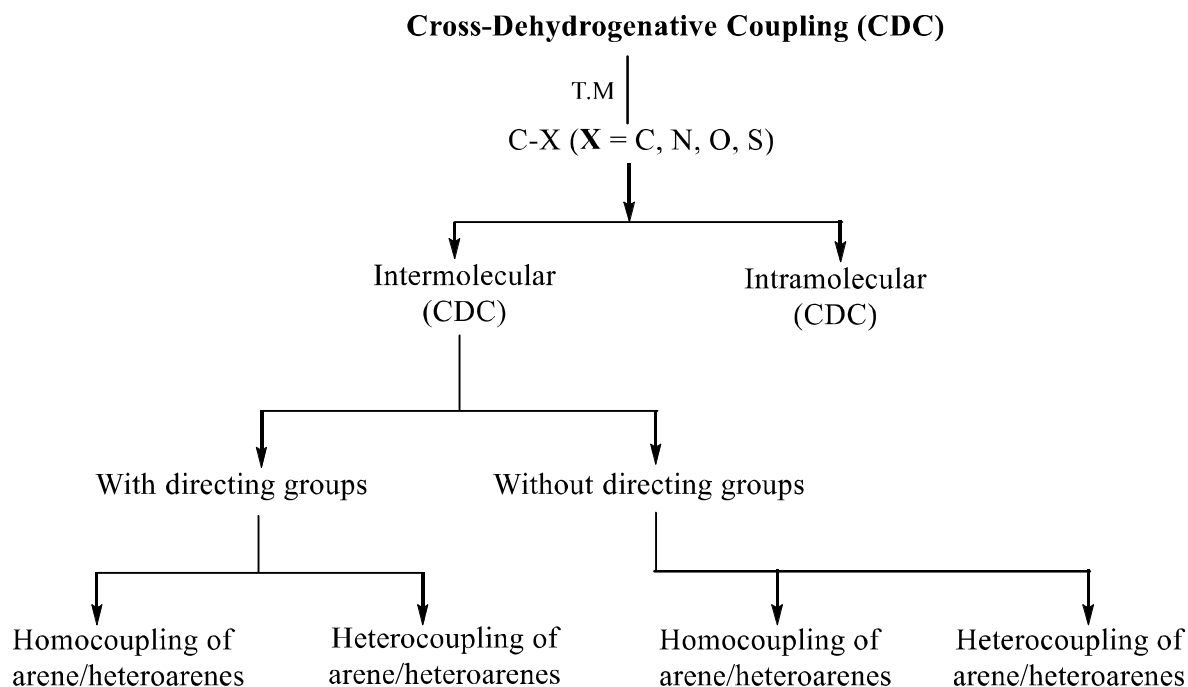


Figure 1.5 Flow chart presentation of cross-dehydrogenative coupling reactions

In this chapter, we mainly focused on the synthesis of bi(hetero)aryls moieties which are typically found in various natural products, pharmaceuticals, and functional materials. Moreover, transition metal-catalyzed synthesis of heteroarenes is of immense importance in organic synthesis. In particular, palladium-catalyzed C–H functionalization is the powerful strategy for the synthesis of bi(hetero)aryls,²⁵ due to the high electrophilicity of metal ions as well as the smooth electropalladation of C–H bonds with palladium. Thus, palladium complexes still dominate in the oxidative coupling between two heteroarenes in the catalytic system. Whereas, selective single C–H bond functionalization within molecules is one of the major challenges related to this methodology. To overcome this challenge, several methodologies have been introduced. Employing directing group on the substrate is one of the most applicable approaches.²⁶ In this, directing group coordinate to the metal center, and the catalyst goes to the closest possible C–H bond to result in high regioselectivity. However, this protocol is mostly used for *ortho*-C–H activation which narrowed the substrate scope, and pre-installation of directing groups is also essential. In this class, non-directed (without directing group) dual C–H activation is the most

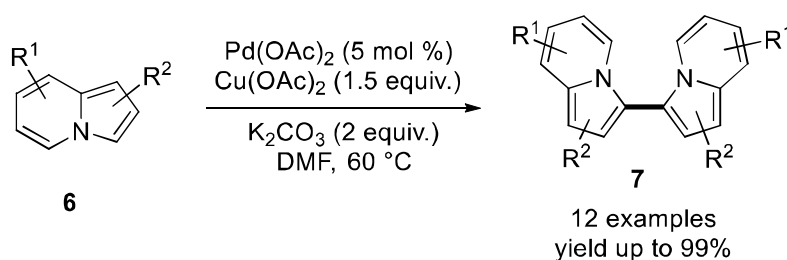
ideal, effective, and straightforward protocol than the directed approach to the synthesis of bi(hetero)aryl compounds (**Figure 1.3**).

During the past decades, palladium-catalyzed cross-dehydrogenative coupling of inactivated (hetero)arenes with simple (hetero)arenes has been explored by a number of groups *via* dual C–H bond activation, but it remains challenging to synthesize bi(hetero)aryl compounds through oxidative cross-coupling reactions.²⁷⁻²⁸ Palladium(II)-catalyzed cross-dehydrogenative coupling for the dimerization of thiophene has been firstly reported by Mori group.²⁹⁻³⁰ Selective homocoupling at C2 position of thiophene (**4**) was achieved in presence of PdCl₂(PhCN)₂ (3 mol %), AgF or AgOCOCH₃ under mild reaction conditions. The protocol provided bithiophene (**5**) derivatives in yield up to 85% (**Scheme 1.2**).



Scheme 1.2 Pd(II)-catalyzed dimerization of thiophene derivatives

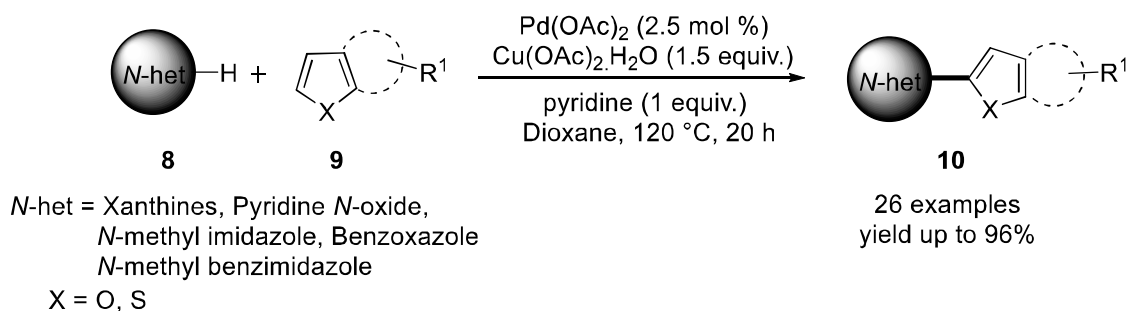
You *et al.* described palladium-catalyzed highly regioselective oxidative homocoupling of indolizines (**6**) to prepare biindolizines (**7**) *via* dual C–H activation. Interestingly, coupling of indazole using Pd(OAc)₂ (5 mol %), Cu(OAc)₂ (1.5 equiv.), K₂CO₃ (2 equiv.) in DMF at 60 °C afforded bisindazolines in yields up to 99%. The method showed broad substrate scope with good regioselectivity. The developed protocol was also utilized for the synthesis of bridged macrobiindolizines in moderate to good yields (34-99%) (**Scheme 1.3**).³¹



Scheme 1.3 Pd(II)-catalyzed synthesis of biindolizine derivatives

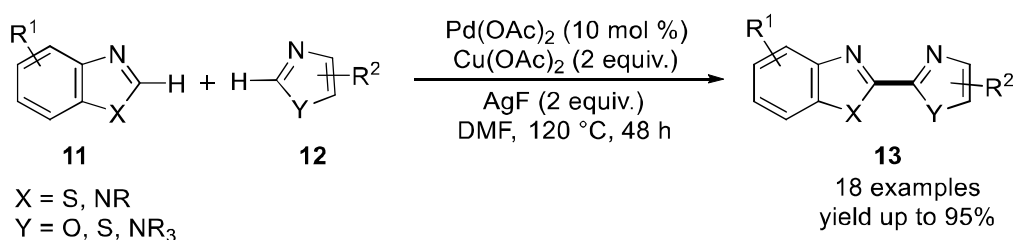
Whereas, oxidative dehydrogenative heterocoupling between two different heteroarenes was not familiar until 2010, because of the regioselectivity, reactivity, and decomposition of heteroarenes issues. You and Hu group disclosed Pd(II)-catalyzed oxidative heterocoupling between *N*-

containing heteroarenes (azoles, pyridine *N*-oxide) (**8**) with five-membered heterocycles (furan, thiophene) (**9**) to afford the broad range of bi(hetero)aryls (**10**) (**Scheme 1.4**). The stoichiometric amount of Cu(I) is act as activator to enhance the reactivity of the azoles, ultimately could promote the C–H activation of azoles. The versatility of the described protocol found broader impact on the construction of unsymmetrical bi(hetero)aryl molecules in material, medicinal and natural product chemistry.³²



Scheme 1.4 Synthesis of biheteroaryls via Pd(II)-catalyzed C–H/C–H coupling

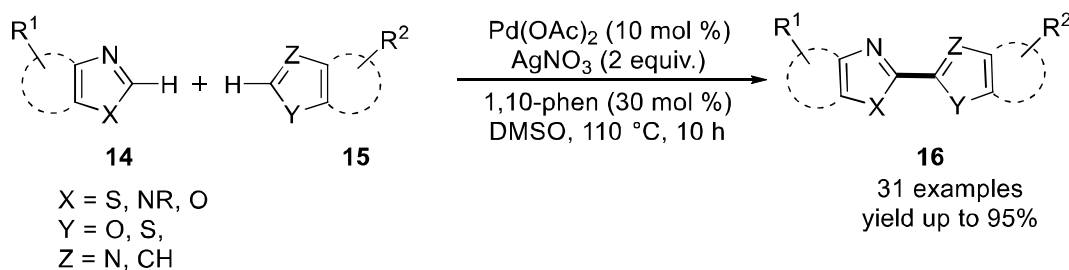
Ofial group reported synthesis of unsymmetrical 2,2'-bi(hetero)aryls (**13**) through palladium(II)-catalyzed selective C–C heterocoupling between the nonfunctionalized benzazoles (**11**) with azoles (**12**). This method employed to the direct access of C2-heteroarylated compounds using benzazoles with N-, O-, and S-containing azoles. Notably, in this reaction homocoupled products formation was suppressed with selective C–H bond cleavage between two heteroarenes to afford bi(hetero)arenes in good to excellent yields (65-95%). (**Scheme 1.5**).³³ The silver and copper salts played pivotal role in this chemical transformations.



Scheme 1.5 Pd(II)-catalyzed dehydrogenative coupling of benzazoles with azoles

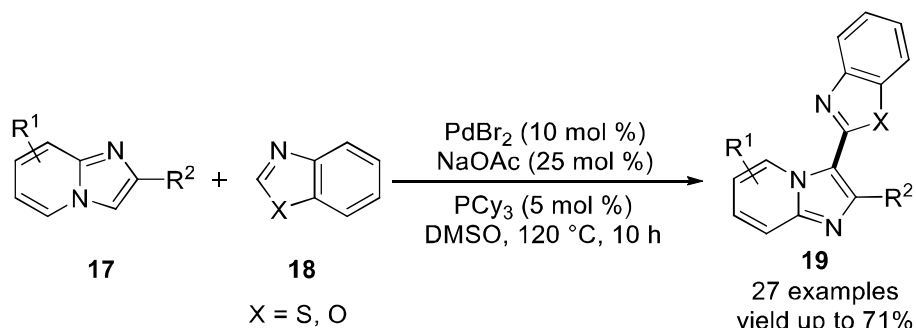
Yang and co-workers developed a Pd(II)-catalyzed oxidative C–H/C–H cross-coupling of benzothiazoles (**14**) with thiophenes and thiazoles (**15**) through two-fold C–H activation to afford the bi(hetero)aryls (**16**) in 11-95% yields. This method allows the cross-coupling between not only electron-rich and electron-deficient carbon centers but also between two different electron-

deficient carbon centers. The deuterium labelling and kinetic isotopic effect (KIE) experiment revealed that the reaction follows CMD pathway and C–H bond cleavage is the rate determining steps. The developed protocol was compatible with a broad range of functional groups and insensitive to air and moisture (**Scheme 1.6**).³⁴



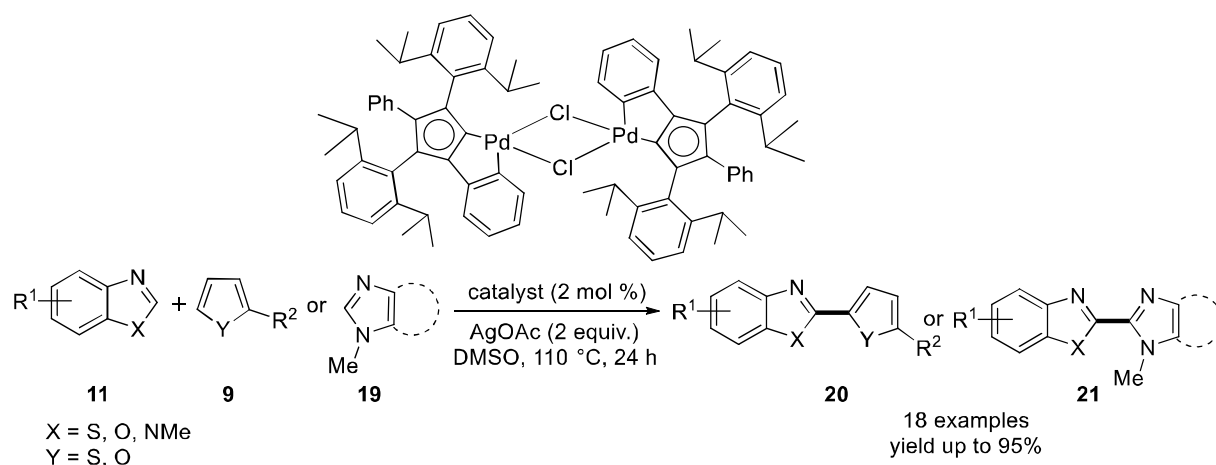
Scheme 1.6 Pd(II)-catalyzed oxidative C–H/C–H coupling of two different heteroarenes

Zhao *et al.* reported the synthesis of 3-azolyl-imidazopyridines (**19**) *via* palladium(II)-catalyzed cross-coupling of imidazopyridines (**17**) with azoles (**18**) using air as the oxidant (**Scheme 1.7**).³⁵ A large number of imidazo[1,2-*a*]pyridine derivatives were smoothly reacted with azoles to furnish the 3-azolyl-imidazopyridine compounds in moderate to good yields (37-71%). The method tolerated various functional groups and showed regioselectivity for C-3/C-2 coupling.



Scheme 1.7 Pd(II)-catalyzed synthesis of 3-azolyl-imidazopyridines

Mandal group utilized the dimeric halo-bridged Pd(II) catalyst bearing an abnormal *N*-heterocyclic carbene backbone for the cross-dehydrogenative coupling of two heteroarenes (**11, 9, 19**) (**Scheme 1.8**).³⁶ Different heterocycles such as *N*-methylimidazole, *N*-methylbenzimidazole, benzothiazole, benzoxazole were coupled with substituted thiophenes, and furfural in good to excellent yields. *In-situ* formed catalytically active acetato-bridged Pd(II) organometallic dimer was trapped and characterized by single X-ray crystallography.



Scheme 1.8 Synthesis of bi(hetero)aryls *via* chloro-bridged palladium dimer catalyst

The reactivity and regioselectivity are the major challenges in the oxidative C–H/C–H cross coupling reactions. As a result, the scientific community has engrossed more attention towards the transition metal organometallic chemistry to resolve these challenges. Organopalladium compounds have attractive synthetic features in organometallic chemistry hence they are exclusively studied for the construction of C–C and C-heteroatom bond formation reactions.³⁷⁻³⁹

1.1.4 Organopalladium Chemistry

The palladium catalysis shows the broad synthetic scope and control the selectivity and reactivity of the synthetic transformations and its outcomes.⁴⁰ Also, high turnover numbers and low catalyst loadings are the desired attributes of the model organopalladium catalyst. The catalytic properties of the metal center in a complex can be fine-tuned by rational design and appropriate choice of the ligands. Generally, the ligands are the requisite part of the transition metal catalyst, which can stabilize the metal center, regulate the selectivity issues of chemical transformations. In this respect, a pincer framework has gained significant attention due to the stability towards moisture and air, and its unique possibility for altering the catalytic activity of metal atoms. The pincer ligands offer notable harmony between reactivity and stability to their metal complexes, where the metal is placed in a protected environment. Since, the first reports from Shaw⁴¹ and van Koten⁴² in the 1970s, a plethora of pincer complexes have been prepared and explored for diverse applications in organic syntheses.⁴³

1.1.5 Classification of Palladacycles

Cyclic palladium complexes incorporating at least one carbon-palladium bond are called palladacycles.⁴⁴⁻⁴⁶ The pincer complexes are the subclass of palladacycles that incorporate two fused palladacycles. The palladacycles can be divided into two types on the basis of donating ability of coordinated atoms: C-anionic four-electron donor (CE) and six-electron donor (ECE). The ECE-type palladacycle is further classified into two types: symmetrical (ECE type) and unsymmetrical type (ECE' type) (**Figure 1.6 a-c**). The CE-type palladacycle (halogen and acetate bridged dimer) is mostly found in two geometric isomers such as *cisoid* and *transoid* conformations (**Figure 1.6 d-e**). Further, the CE-type palladacycles distinguished depending upon the nature of X-type ligands like neutral (dimer,⁴⁷ bis-cyclopalladated,⁴⁸ or monomeric⁴⁹), cationic, or anionic⁵⁰ (**Figure 1.7**). Similarly, ECE-type of palladacycles are classified into 3 types: symmetrical,⁵¹⁻⁵³ unsymmetrical⁵⁴⁻⁵⁶ and mixed contains the different metallated carbon (sp^2 and sp^3) and ring size (five, six-membered rings)⁵⁷⁻⁵⁹ (**Figure 1.8**).

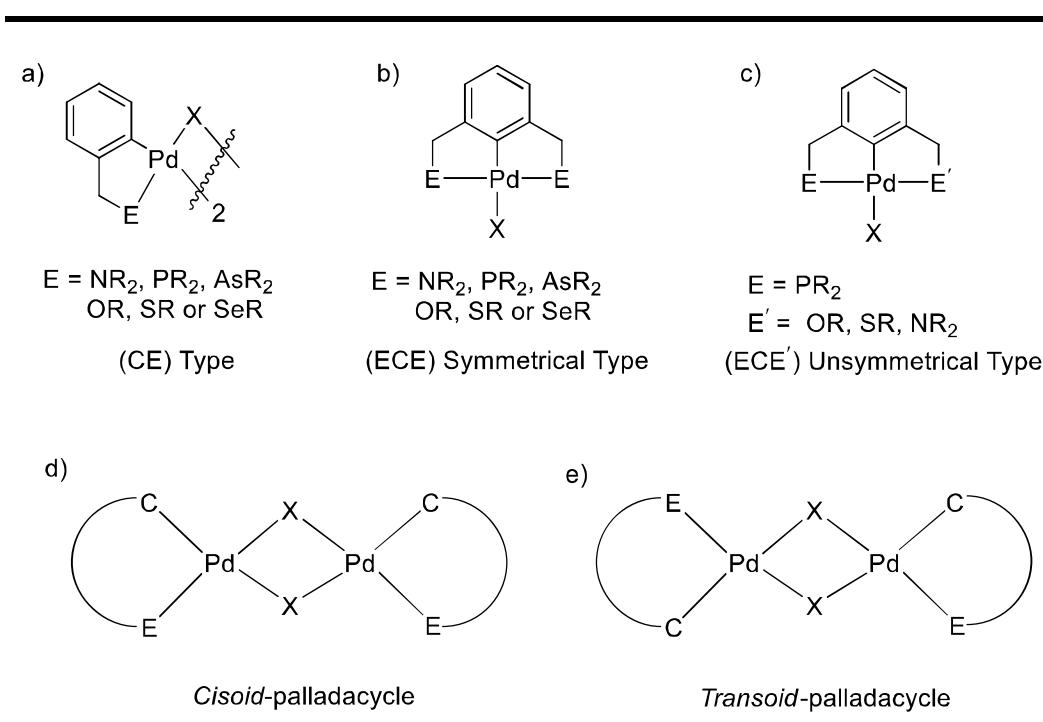


Figure 1.6 Classification of palladacycle

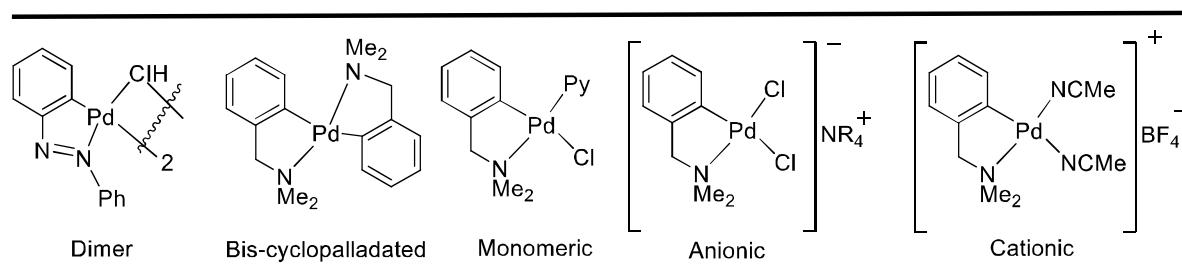


Figure 1.7 Examples of CE palladacycle

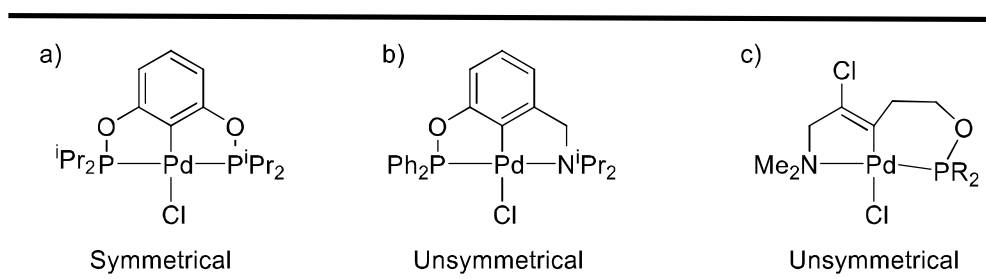


Figure 1.8 Examples of ECE palladacycle

The classification of the various pincer ligands is based upon the coordination of three atoms to the metal center, generally abbreviated as ECE. For example, a complex (Scheme 1.6b) side arm with phosphine ligands ($E = \text{PR}_2$) then would be called as PCP complex and with amino ligands ($E = \text{NR}_2$) a NCN complex. The refinement in coordination sites (N/O/S/P) of the palladium atom is the most significant features of palladium pincer complexes. Since the meridional orientation of the pincer ligands is coplanar, the steric and electronic properties of the pincer ligands strongly affect the palladium center in catalysis. A suitable choice of the chelating arm (E) of the pincer ligands, like different donor groups, has effectively influenced the reactivity of the pincer complex. Likewise, the chiral moiety on the side arm of pincer ligands provides numerous applications in asymmetric synthesis. Furthermore, the accessibility of the reactive site of the palladium can be fine-tuned by steric factors. The electronic effects of the pincer complex can be controlled with the substitution of electron-deficient or -rich character on the *para* position of the aryl group (Figure 1.9).⁶⁰

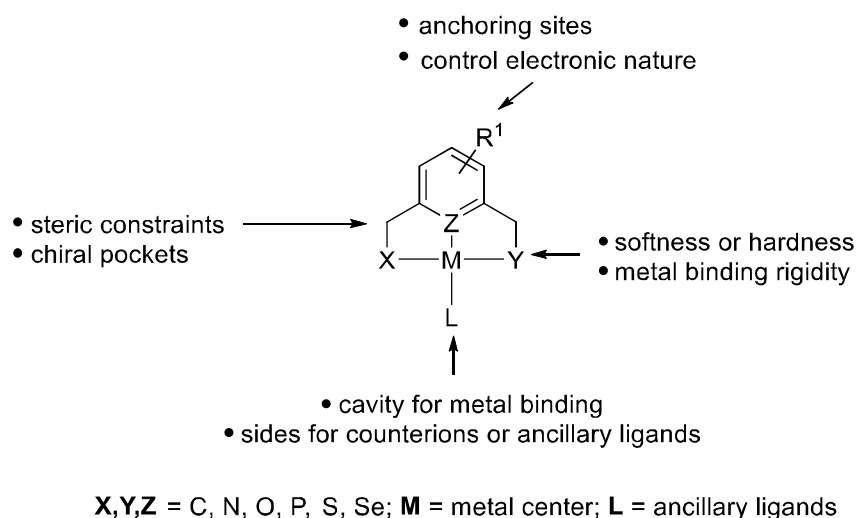
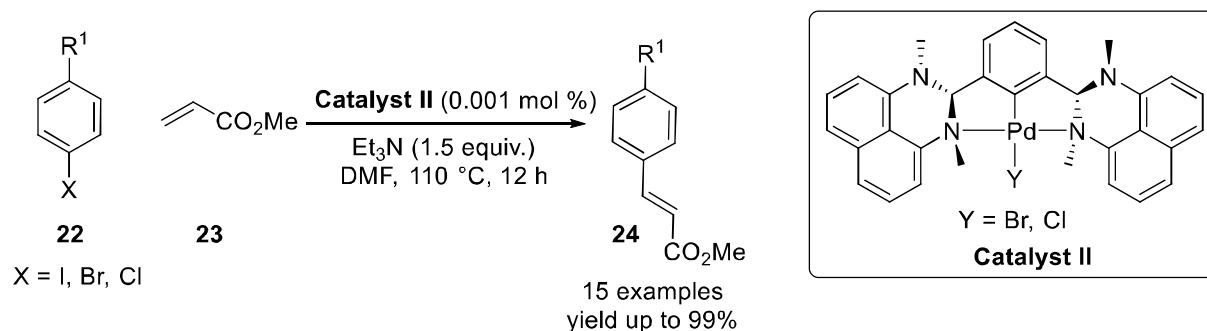


Figure 1.9 Pincer ligands sites and their effects on the properties of the metal center

Because of its some attractive features like easy handling and preparation, insensitive toward the air and moisture as well as efficient tunability make these complexes more convenient.⁶¹ Moreover, the design and development of low-cost and high-efficiency palladium pincer complexes is an area of great interest in organometallic chemistry.

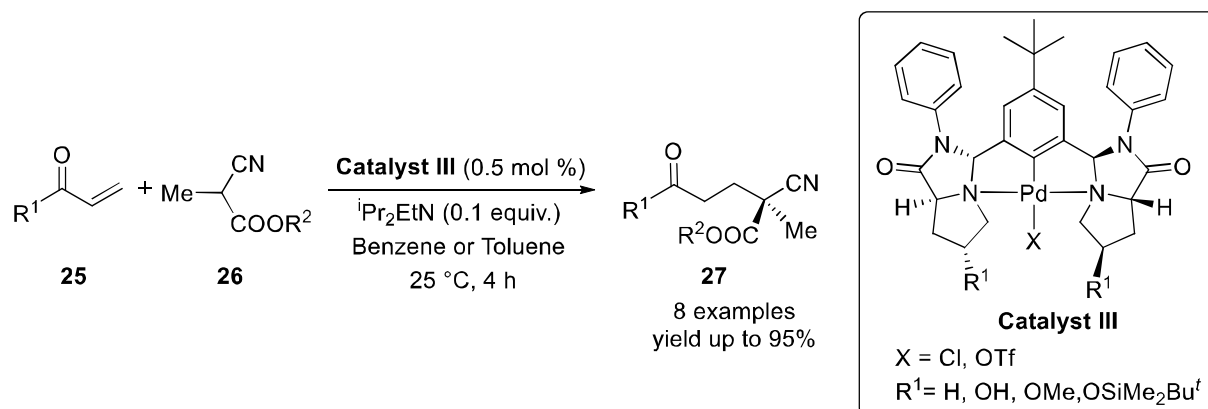
In this chapter, we have discussed the carbon and nitrogen-containing palladium-based pincer complexes and their catalytic applications in organic synthesis. Chung group described synthesis of a new palladium NCN pincer complex (**Catalyst II**). Additional *N*-coordinating sides and temperature-dependent behavior of the **catalyst II** makes it more attractive and reactive towards synthetic applications. The catalytic activity and stability of the complex was investigated in the Heck reaction and it resulted up to 99% yield of Heck product (**Scheme 1.9**).⁶²



Scheme 1.9 Synthesis of Heck coupled products using Pd(II) NCN pincer complex

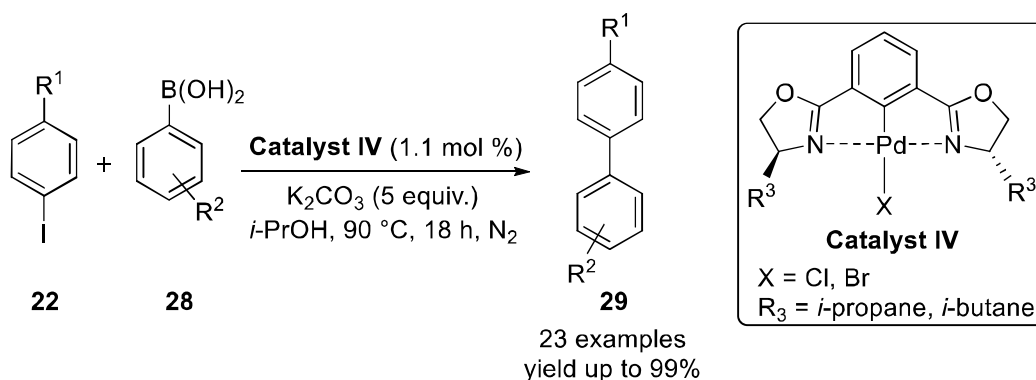
Uozumi *et al.* developed the novel palladium NCN pincer complex having chiral hexahydro-1*H*-pyrrolo[1,2-*c*]imidazolone groups. The chiral pincer complex was used for the synthesis of 2-

cyano-2-methyl-oxoheptanoate (**27**) via catalytic asymmetric Michael addition of isopropyl 2-cyanopropionate (**26**) to ethyl vinyl ketone (**25**) with 83% (ee) enantioselectivity (**Scheme 1.10**).⁶³



Scheme 1.10 Synthesis of 2-cyano-2-methyl-oxoheptanoate derivatives using palladium chiral pincer complex

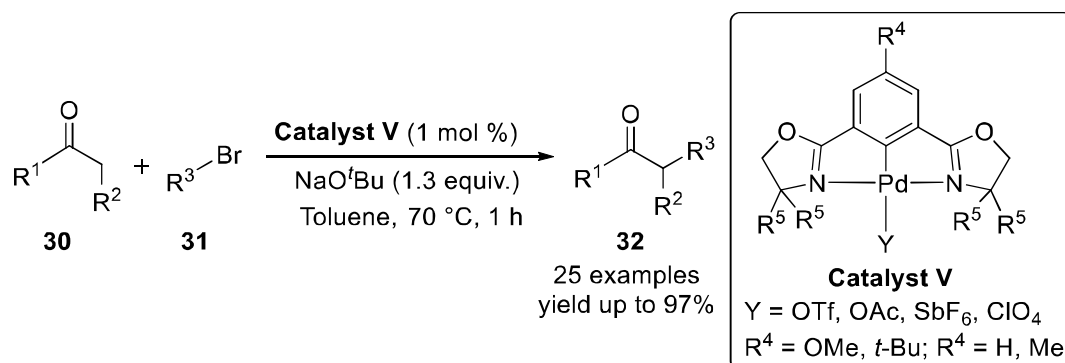
Nishiyama and co-workers demonstrated the synthesis of bis(oxazolinyl)phenyl-palladium(II) pincer complex and its catalytic application for the Suzuki-Miyaura coupling reactions.⁶⁴ The reaction of boronic acids (**28**) and aryl halides (**22**) in presence of phenox-Pd(II) pincer complex (**catalyst IV**) afforded the coupled products (**29**) in high yields with moderate enantioselectivity. The catalyst exhibited over 900,000/s TON and 45,000/s TOF. The mechanism of the cross-coupling reaction followed Pd(II) to Pd(IV) catalytic cycle, which is different from other pincer catalysts such as PCP, SCS and SCN systems (**Scheme 1.11**).



Scheme 1.11 Synthesis of biaryl compounds using phebox-Pd(II) complexes

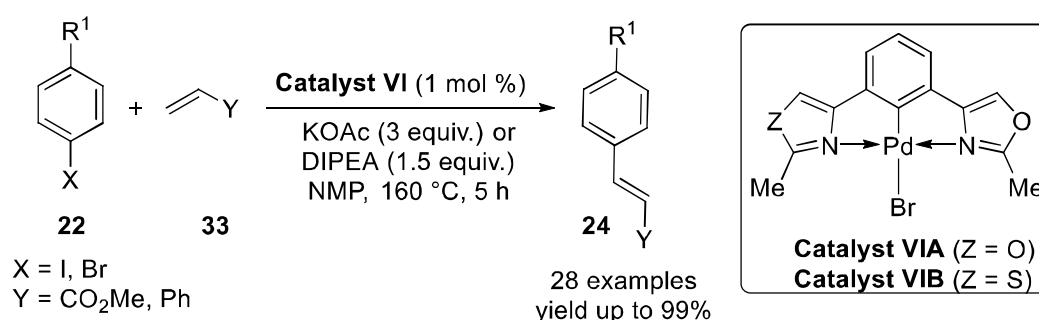
Connell group synthesized a highly reactive, air and water-stable, NCN-Pd(II) pincer complex (**catalyst V**). The **catalyst V** was utilized for the selective α -arylation of ketone (**30**) with various aryl bromides (**31**).⁶⁵ The advantages of this methodology were the low catalyst loading (1 mol

%), formation of desired products in a short duration of time (1 h), and suitable reaction temperature (70 °C). Moreover, readily available substrates and exclusively synthesis of the monoarylated products made this reaction more convenient (**Scheme 1.12**).



Scheme 1.12 Selective synthesis of α -arylated compounds through the novel (NCN)-Pd(II) pincer complexes

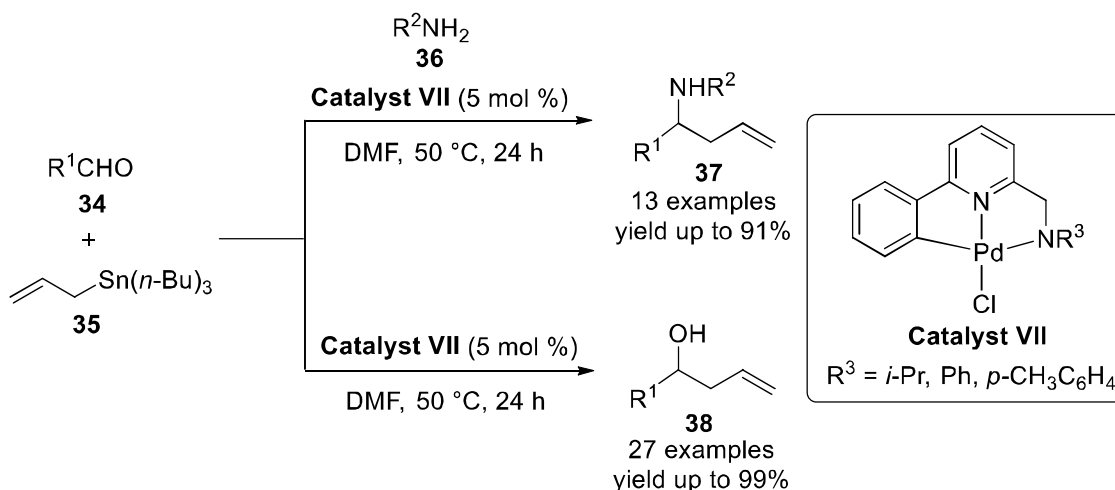
Xiao *et al.* reported the synthesis of two NCN pincer ligand containing oxazol-4-yl and thiazol-4-yl frameworks, which underwent palladation to furnish the two new bis(azole) pincer complexes (**Catalyst VIA and VIB**).⁶⁶ The synthesized NCN pincer complexes were fully characterized by NMR, LCMS, DSC-TGA, and single-crystal X-ray diffraction. The catalysts are thermally stable in both solid and solution phases and also sustain the stability for long term. Further, the catalysts were utilized in the Mizoroki-Heck coupling reactions under mild reaction conditions with short reaction time even under open-air to afford cross-coupling products in good to excellent yields (**Scheme 1.13**).



Scheme 1.13 Investigation of Mizoroki-Heck reaction using Pd(II) bis(azole) pincer catalysts

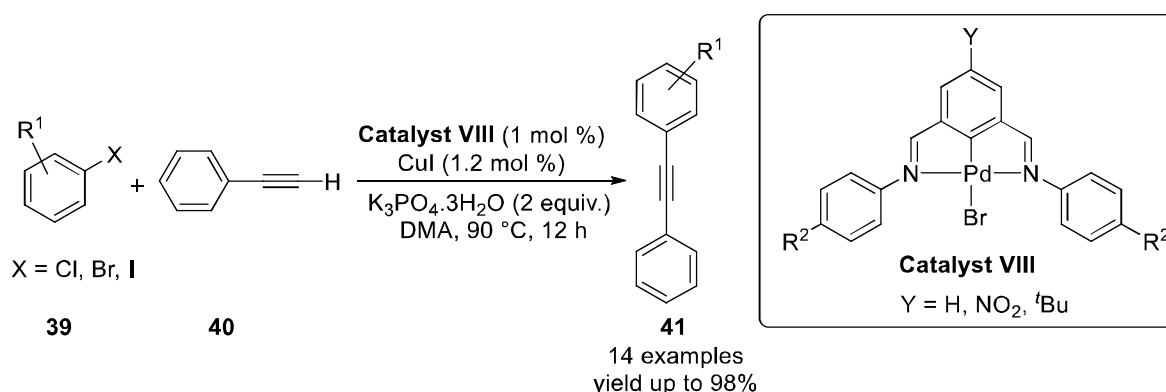
Song and co-workers reported the synthesis of CNN pincer Pd(II) complexes (**Catalyst VII**) by using *N*-substituted-2-aminomethyl-6-phenylpyridines as ligand. The synthesized Pd(II) complexes were explored for the allylation of substituted aldehydes (**34**), allyltributyltin (**35**) and,

arylamines (**36**). The homoallylic amines (**37**) and alcohols (**38**) were synthesized in good to excellent yields. Also, it is observed that CNN Pd(II) pincer complexes exhibit higher reactivity towards allylation reaction than related NCN Pd(II) pincer complexes (**Scheme 1.14**).⁶⁷



Scheme 1.14 Synthesis of homoallylic alcohols and amines *via* CNN pincer Pd(II) complexes

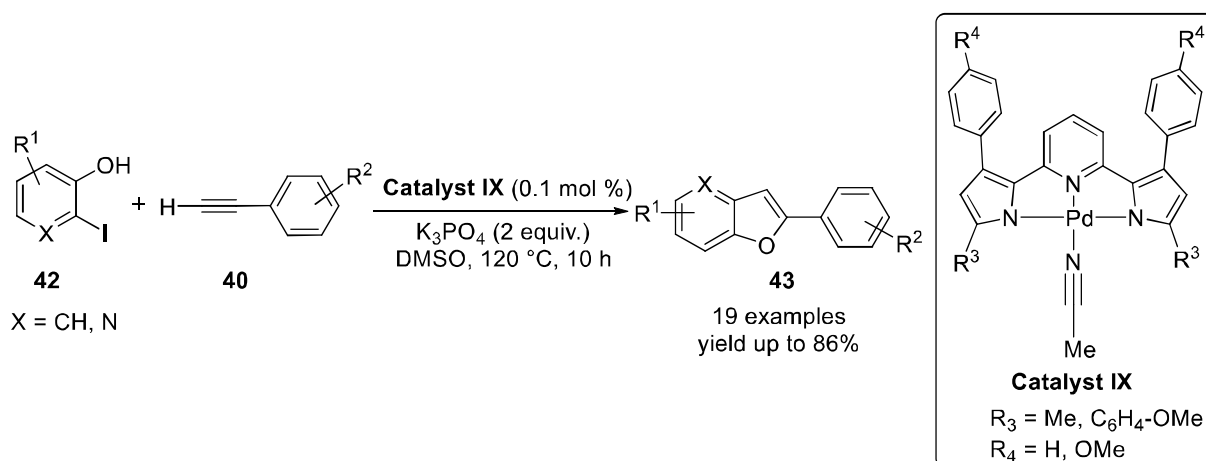
Wang group synthesized a palladium (II)-pincer complex (**Catalyst VIII**) for the reaction of isophthalaldehydes with anilines, which underwent palladation with NCN diamine ligands.⁶⁸ The Pd pincer complex and its precursors were characterized by elemental analysis, NMR, and IR spectroscopy. The obtained complexes were studied for Sonogashira coupling reaction. Interestingly, the *para* substituent on the phenyl ring was responsible for the reactivity of the complex to afford the coupled products (**41**) in good to excellent yields (**Scheme 1.15**).



Scheme 1.15 Synthesis of alkynes using NCN pincer Pd(II) complexes

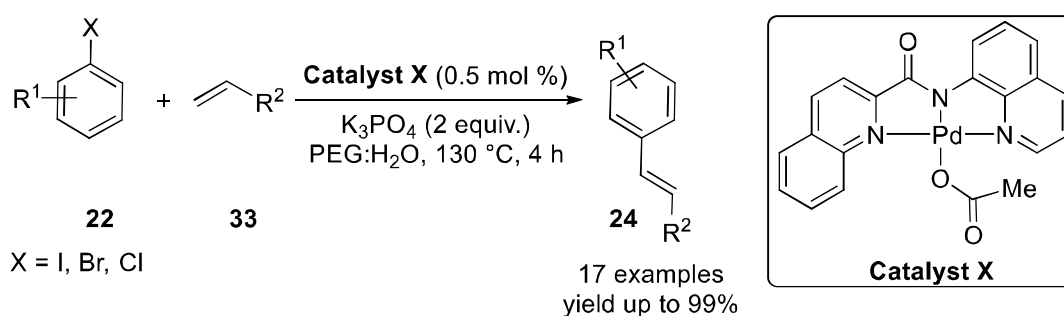
Dash and co-workers reported the 2,6-bis(pyrrolyl)pyridine ligand framework for the synthesis of palladium pincer complexes (**Catalyst IX**).⁶⁹ The well-defined palladium-pincer complexes were

explored for the one-pot tandem Heck alkynylation followed by cyclization reactions to afford the benzofuran derivatives (**43**) in moderate to good yields. The silent features of the designed protocol are the low catalyst loading (0.1 mol %) and open-air environment for reaction. Notably, the temperature and solvents were affecting the reactivity of the pincer complexes and ultimately it helped to increase the yield of cyclized products (**Scheme 1.16**).



Scheme 1.16 Synthesis of benzofuran derivatives using NNN pincer Pd(II) complexes

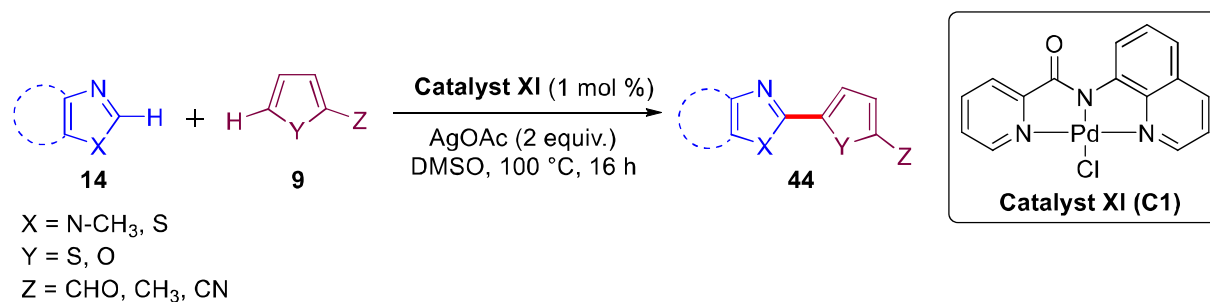
Bagherzadeh group reported synthesis of 8-(2-quinoline carboxamide)quinoline (Hqcq) as a three-dentate carboxamide ligand, which was further used in synthesis of palladium complex Pd(II)(qcq)(OAc) (**Catalyst X**).⁷⁰ This complex was investigated for the typical Mizoroki-Heck coupling reactions of aryl halides (**22**) with alkenes (**33**) to furnish the coupled products (**24**) in 11-99% yields (**Scheme 1.17**).



Scheme 1.17 Synthesis of Mizoroki-Heck coupled products *via* Pd(II)(qcq)(OAc) catalyst

The earlier reported protocols for cross-dehydrogenative coupling reactions suffer from drawbacks such as (i) high catalyst loading (>2 mol % Pd), (ii) long reaction times and high reaction temperature (~120–140 °C), (iii) indiscriminant of homo- or heterocoupled products, (iv) limited

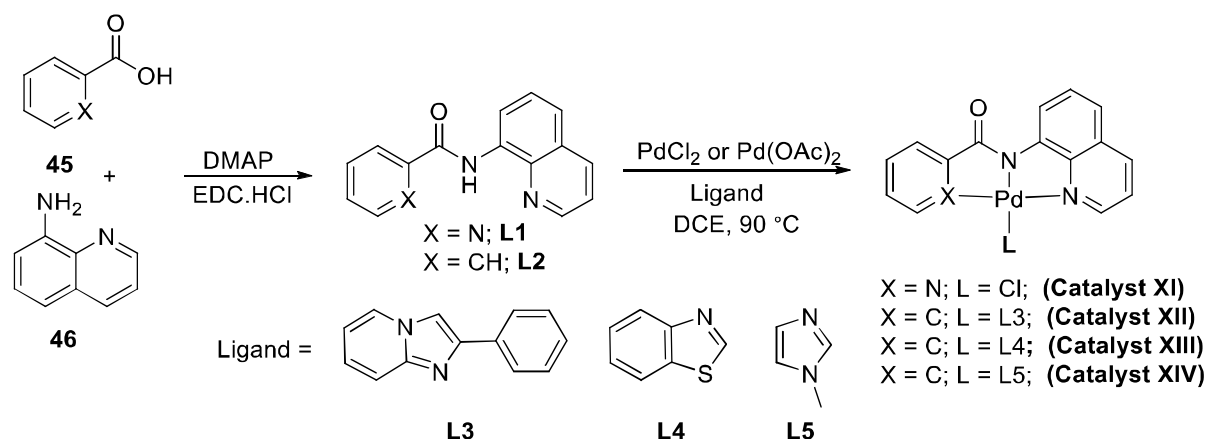
substrate scope, (v) low functional group tolerance, and (vi) lack of reusability of the catalyst. Thus there is a need to develop a simple and efficient synthetic protocol for coupling of (hetero)arenes. In this chapter, we have synthesized novel palladium complexes of NNN or CNN pincer ligands (**XI–XIV**) and explored their catalytic application for cross-dehydrogenative coupling (CDC) reactions of heteroarenes under mild reaction conditions with low catalyst loading (1.0 mol %, **Scheme 1.18**).



Scheme 1.18 Pd(II) NNN/CNN pincer catalyzed synthesis of bi(hetero)aryl compounds

1.2 RESULTS AND DISCUSSION

The ligands (**L1** and **L2**) were synthesized by the reaction of 8-aminoquinoline with benzoic acid or picolinic acid, respectively in the presence of 4-dimethylaminopyridine (DMAP) and 1-ethyl-3-(3-dimethylaminopropyl)carbodiimide hydrochloride (EDC·HCl).⁷¹ The complex **XI** was synthesized by the reaction of *N*-(quinolin-8-yl)picolinamide (**L1**) and PdCl₂ (1 equiv.) in DCE at 65 °C for 12 h (**Scheme 1.19**). Likewise, treatment of *N*-(quinolin-8-yl)benzamide (**L2**, 1 equiv.) and different ligands *viz* 2-phenylimidazo[1,2-*a*]pyridine (**L3**, 1 equiv.), benzothiazole (**L4**, 1 equiv.) and 1-methyl-1*H*-imidazole (**L5**, 1 equiv.) with Pd(OAc)₂ (1 equiv.) under similar reaction conditions resulted complexes **XII–XIV** as yellow solid (**Scheme 1.19**). *In-situ* formation of similar CNN type Pd-pincer complexes have been observed in palladium-catalyzed directed C–H functionalization of *N*-quinolyl benzamides.^{72–74}



Scheme 1.19. Syntheses of palladium complexes **XI-XIV**.

The ^1H NMR, $^{13}\text{C}\{^1\text{H}\}$ NMR, IR and HRMS data of the complexes **XI-XIV** were well in agreement with the structures. In the ^1H NMR spectra of complexes **XI-XIV**, the missing NH signal of **L1** and **L2** at 10.73 and 12.27 ppm confirmed the coordination of Pd with amidic nitrogen of ligand. Moreover, the missing aromatic ring proton signal in catalyst **XI-XIV** further revealed that the activation of C–H bond of aromatic ring through palladium precursor, forming a five membered palladacycle ring. In the $^{13}\text{C}\{^1\text{H}\}$ NMR spectra of catalyst **XI-XIV**, the C=O signal appeared in the range of 166.4-177.9 ppm which was deshielded by 4-12 ppm with respect to the free ligands. In the IR spectra of catalyst **XI-XIV** peaks corresponds to amidic C=O stretching frequency appeared around 1604-1635 cm^{-1} . In HRMS of catalyst **XI**, the peak at m/z 353.9845 appeared due to $[\text{M} - \text{Cl}]^+$ ion, for **XII** the peak at m/z 547.0742 corresponds to $[\text{M} + \text{H}]^+$ ion, for **XIII** peak at m/z 352.9903 corresponds to $[\text{M} - \text{L} + \text{H}]^+$ while for **XIV** peak at m/z 391.4953 corresponding to $[\text{M} - \text{L} + \text{K}]^+$ ion. Further, structures and bonding of catalyst **XI-XIII** were also authenticated with the help of single crystal X-ray diffraction (**Figure 1.14**). Complex **XI-XIV**, were found to be stable in air and moisture and can be stored at room temperature for more than three months. All the four newly synthesized complexes were found to be highly soluble in solvents like CH_2Cl_2 , CHCl_3 , CH_3CN , DMF, DMSO, MeOH and sparingly soluble in solvents like *n*-hexane, *n*-pentane, and diethyl ether. The ^1H and $^{13}\text{C}\{^1\text{H}\}$ NMR spectra of synthesized catalyst **XI-XIV** are given below in **Figures 1.10-1.13**.

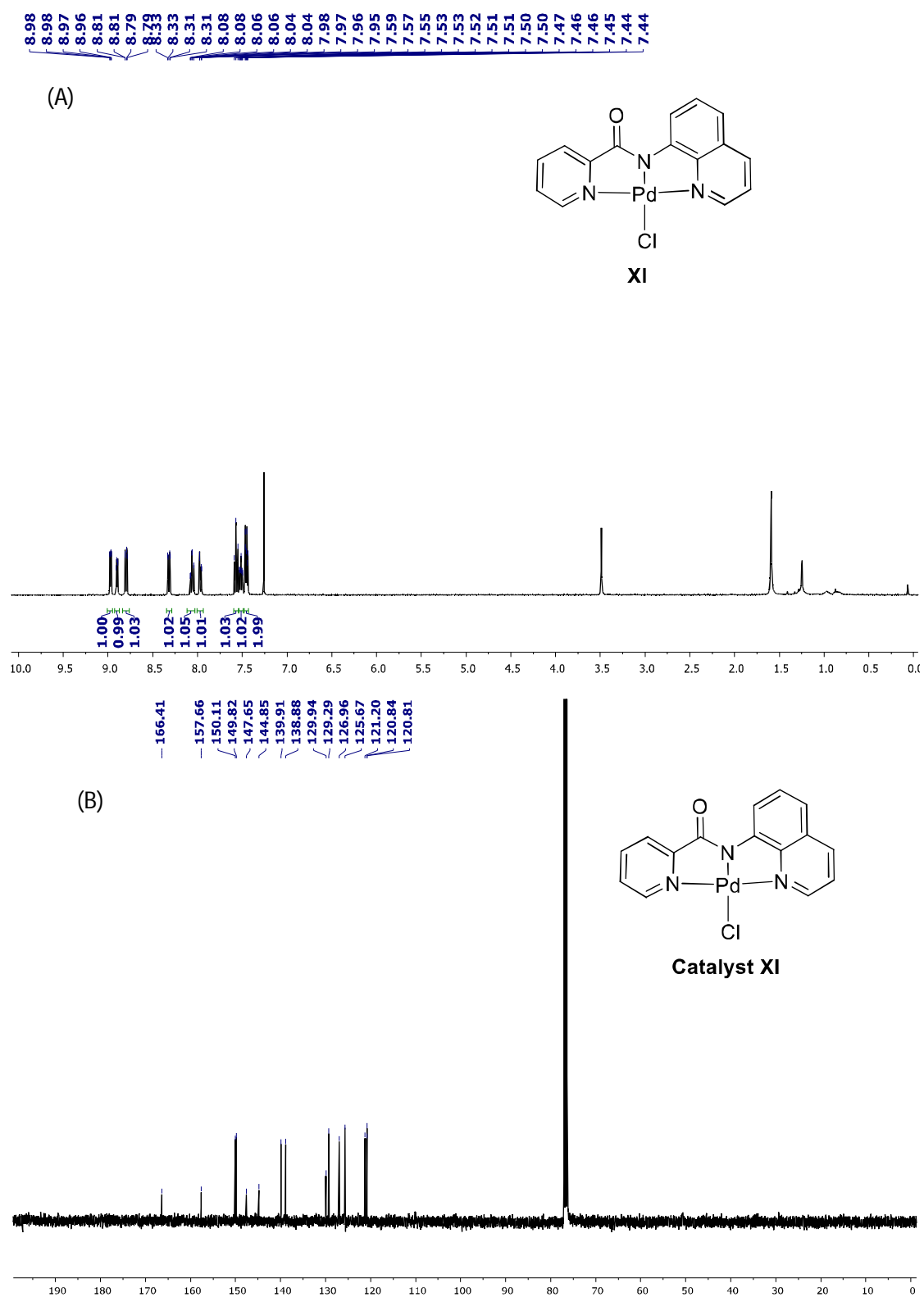


Figure 1.10: (A) ^1H NMR and (B) $^{13}\text{C}\{^1\text{H}\}$ NMR spectra of complex XI in CDCl_3 .

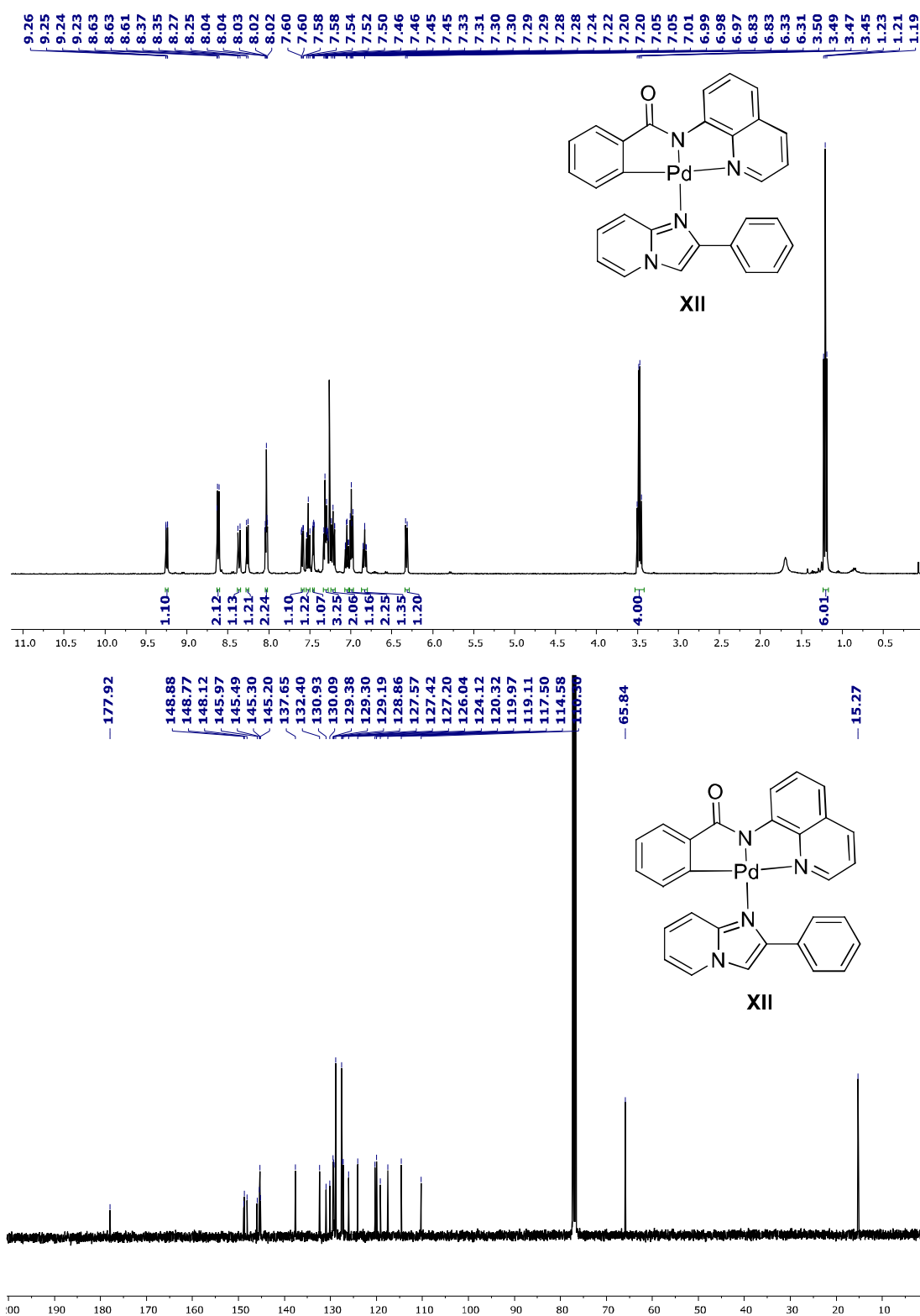
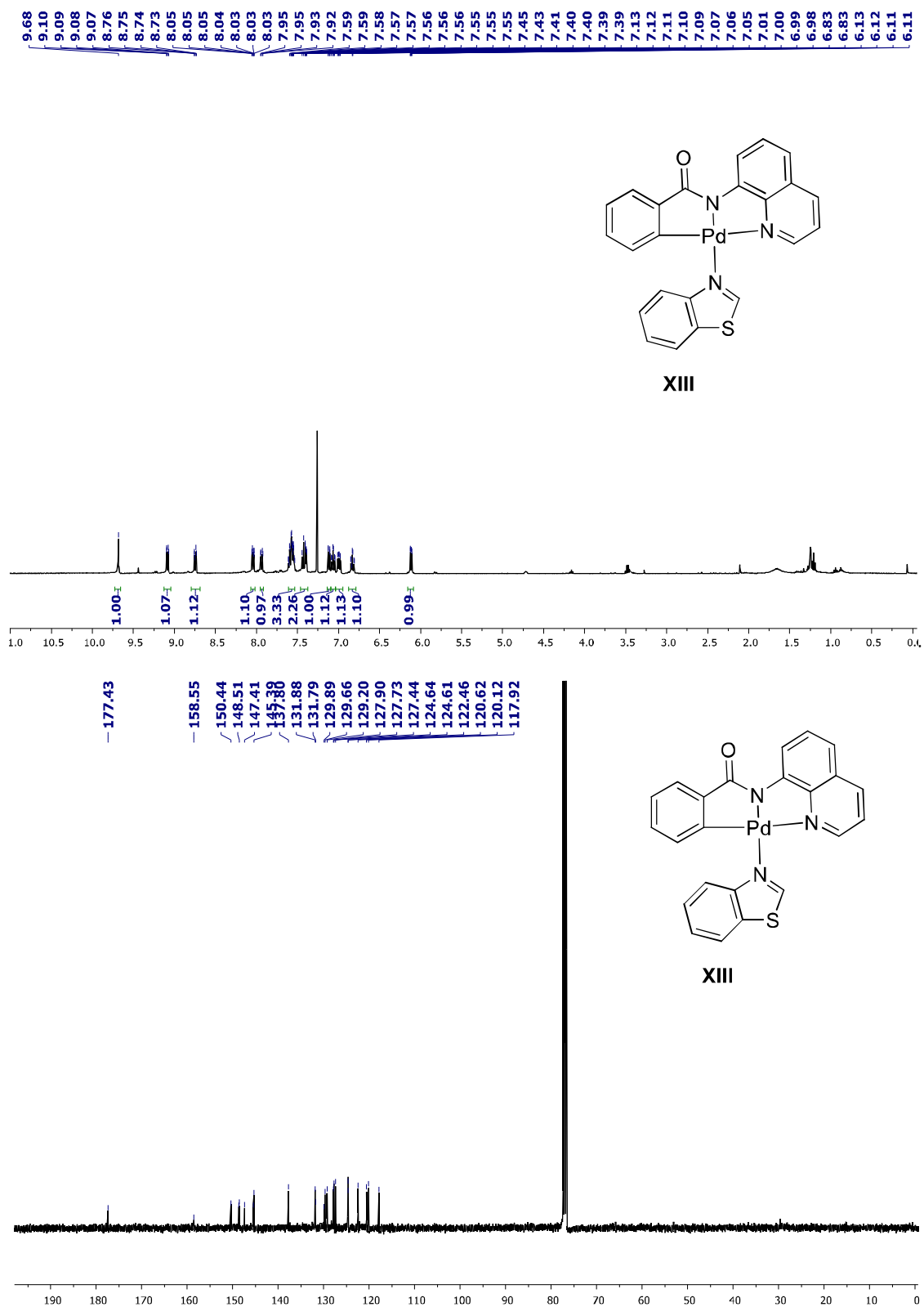


Figure 1.11: ^1H NMR and $^{13}\text{C}\{^1\text{H}\}$ NMR spectra of complex XII (complex trapped diethyl ether) in CDCl_3 .

Figure 1.12: ^1H NMR and $^{13}\text{C}\{^1\text{H}\}$ NMR spectra of complex XIII in CDCl_3 .

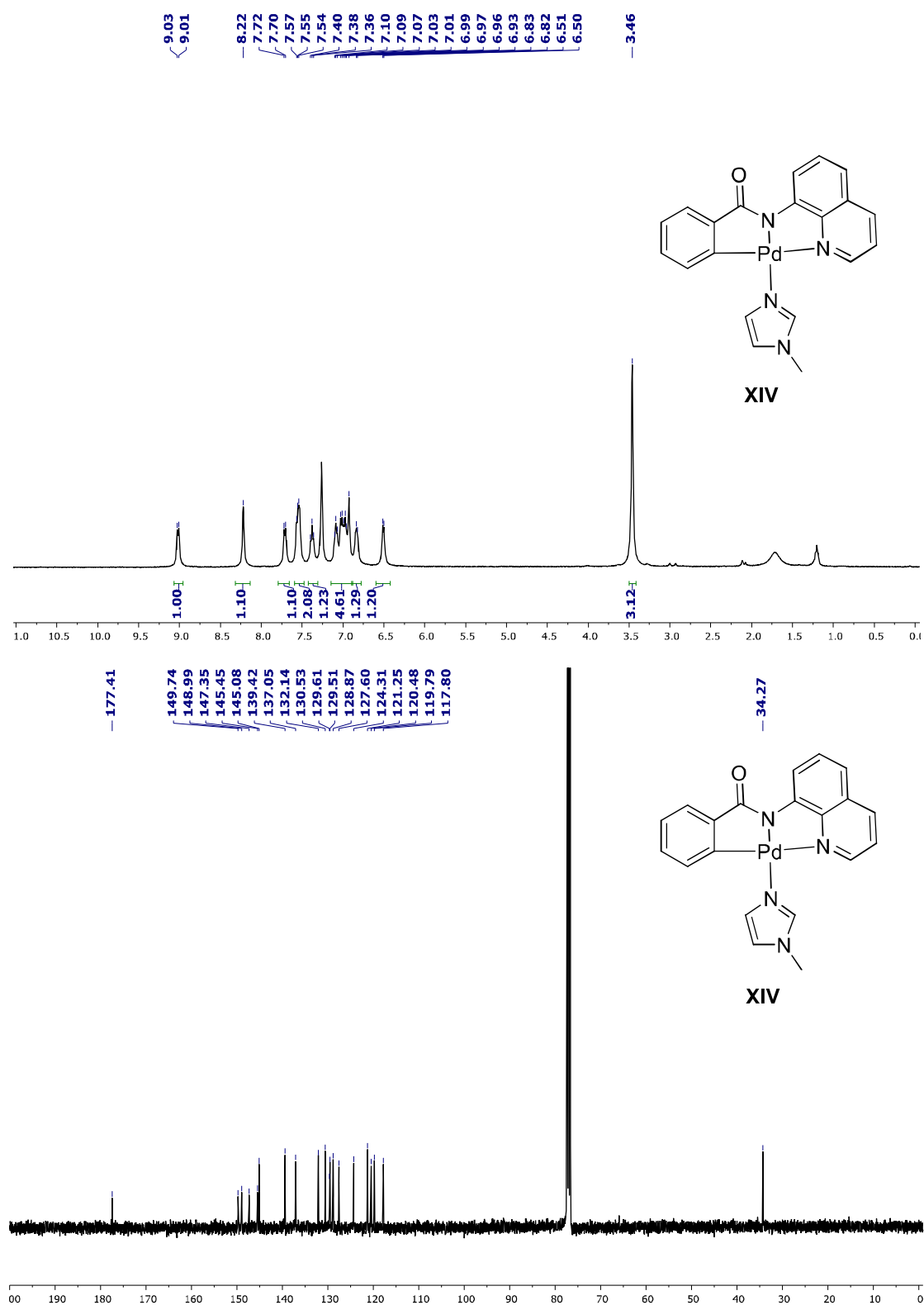


Figure 1.13: ^1H NMR and $^{13}\text{C}\{^1\text{H}\}$ NMR spectra of complex XIV in CDCl_3 .

1.2.1 Crystal Structures

A CH₃CN solution of **XI** and CHCl₃/hexane solution of **XII** and **XIII** were used to grow the X-ray quality crystals under ambient conditions. The repeated attempts to crystallize the complex **XIV** were unsuccessful. Molecular structures of **XI-XIII** are shown in **Figures 1.12**. Crystal structure data and refinement parameters of **XI-XIII** are shown in **Table 1.3**. In all three complexes palladium has a distorted square planer geometry and bond angles around Pd are near to 90 and 180°. Palladium is coordinated with ligand in tridentate fashion through N-N-N or C-N-N coordination mode, forming two five membered rings. The Pd–N bond length of amidic nitrogen in **XI-XIII** are 2.001(2), 1.980(3) and 1.970(4) Å, respectively, which are consistent with literature reported amidic palladium complexes (2.008-2.014(3) Å).⁷⁵ Pd–N (quinoline nitrogen) bond length are 2.014(2), 2.123(3) and 2.102(4) Å, respectively, consistent with reported neutral Pd–N bond lengths (2.005-2.035(3) Å).⁷⁶ The Pd–C bond distances in **XII**, **XIII** are 1.998(4) and 1.983(5) Å, respectively, which are similar to the values 1.979(4) Å reported earlier for palladacycle complex.⁷⁷ Complex **XI** contains 4 molecules in its unit cell but we have not observed any solvent molecule in the unit cell whereas complex **XII** has four molecules in its unit cell with four solvated CHCl₃ molecules and complex **XIII** has only two molecules in unit cell with two solvent molecules.

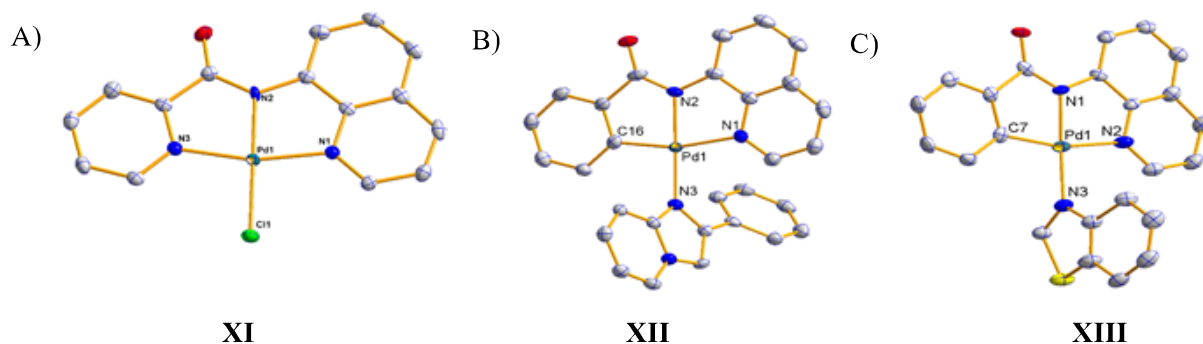


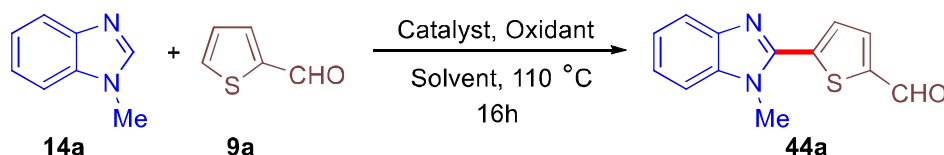
Figure 1.14: a) Molecular structure of **XI**, b) Molecular structure of **XII**, c) Molecular structure of **XIII**.

1.2.2 Cross-Dehydrogenative Coupling Reaction of Heteroarenes

Reaction of *N*-methylbenz-imidazole (**14a**, 1 equiv.) with 2-formylthiophene (**9a**, 4 equiv.) in the presence of palladium complexes **XI-XIV** (1.0 mol %) to give 5-(1-methyl-1*H*-benzo[*d*]imidazol-

2-yl)thiophene-2-carbaldehyde (**44a**) was studied as model reaction for the optimization of the reaction conditions for cross dehydrogenative coupling reaction of heteroarenes (**Table 1.1**).

Table 1.1: Optimization of reaction conditions for cross-dehydrogenative coupling reaction of heteroarenes^a



| Entry No. | Catalyst | Oxidant | Solvent | Yield ^b (%) |
|-----------------|-----------------------|--|---------|------------------------|
| 1 | XI | Ag ₂ CO ₃ | DMSO | 42 |
| 2 | XI | Ag ₂ O | DMSO | 32 |
| 3 | XI | Cu(OAc) ₂ ·H ₂ O | DMSO | nd |
| 4 | XI | AgOAc | DMSO | 66 |
| 5 | XI | AgNO ₃ | DMSO | 18 |
| 6 | XI | AgOAc | DMA | 53 |
| 7 | XI | AgOAc | DMF | 51 |
| 8 | XI | AgOAc | NMP | 29 |
| 9 | XI | AgOAc | THF | 14 |
| 10 ^c | XI | AgOAc | DMSO | 52 |
| 11 ^d | XI | AgOAc | DMSO | 41 |
| 12 | - | AgOAc | DMSO | nd |
| 13 | XI | - | DMSO | nd |
| 14 ^e | XI | AgOAc | DMSO | 40 |
| 15 | XI^f | AgOAc | DMSO | 68 |
| 16 | XI^g | AgOAc | DMSO | 28 |
| 17 | XI^h | AgOAc | DMSO | 13 |
| 18 | XII | AgOAc | DMSO | 63 |
| 19 | XIII | AgOAc | DMSO | 61 |
| 20 | XIV | AgOAc | DMSO | 58 |

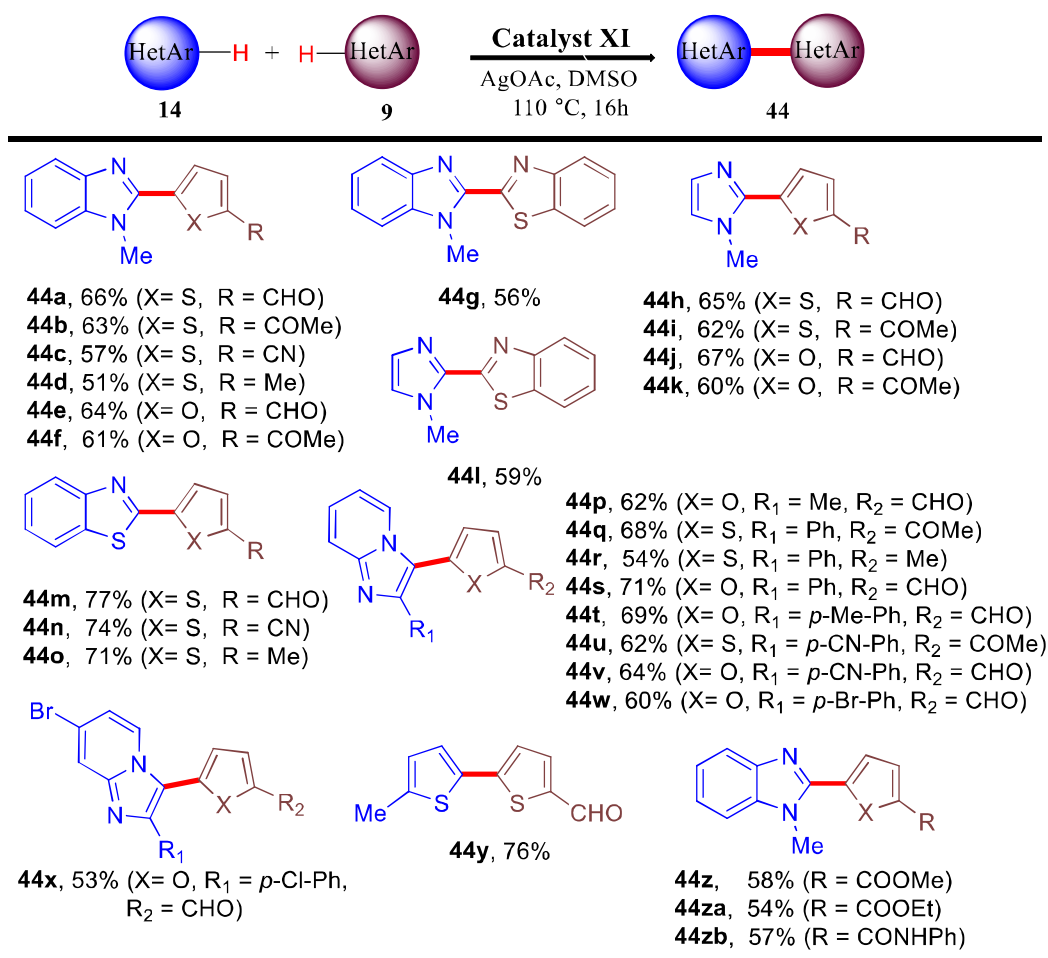
^aReaction conditions: **14a** (0.757 mmol), **9a** (3.030 mmol), catalyst (1.0 mol %), oxidant (1.5 equiv.), solvent (3 mL). ^bIsolated yield. ^cat 80 °C. ^dat 140 °C. ^e1 equiv. of **14a** was used. ^f2 mol% of **XI** was used. ^g0.5 mol % of **XI** was used. ^h0.1 mol % of **XI** was used. nd = not determined.

Initially, several oxidants were screened and among all use of AgOAc yielded highest yield (66%) of **44a** (**Table 1.1**, entries 1–5). Next, various solvents were screened and DMSO was found to be the most suited solvent yielding **44a** in 66% (**Table 1.1**, entry 4), whereas solvents like, DMA, DMF, NMP and THF resulted **44a** in 53%, 51%, 29% and 14% yield, respectively (**Table 1.1**, entries 6–9). Reaction in the absence of catalyst or oxidant did not result in the formation of

coupled product **44a** (Table 1.1, entry 12, 13). Use of lower amount of **9a** (1 equiv. instead of 4 equiv.) gave only 40% yield of **44a** along with 21% of homocoupled product **45a** (Table 1.1, entry 14). Similar results have been observed previously and one of the reaction partner is used in excess in order to avoid homocoupled product.³² The choice of catalyst and catalyst loading were subsequently screened (Table 1.1, entry 15-19). No significant improvement in the yield of **44a** was observed on increasing the catalyst loading of **XI** to 2.0 mol % (Table 1.1, entry 15). On lowering the catalyst loading of **XI** to 0.5 and 0.1 mol %, the yield of **44a** reduced significantly to 28% and 13%, respectively (Table 1.1, entry 16 and 17). Finally, model reaction was performed using catalysts **XI-XIV** and **44a** was obtained in 63%, 61% and 58% yield, respectively (Table 1.1, entry 18-20). Best yield of **44a** was obtained using **XI** (1.0 mol %) in the presence of AgOAc in DMSO at 110 °C (Table 1.1, entry 4) and it was selected as standard conditions for further substrate scope evaluation.

With the optimal reaction conditions in hand, the scope and generality of the developed protocol was evaluated for variety of structurally divergent heterocycles and the results are presented in Table 1.1. It is noticeable that the reaction with all heteroarenes went smoothly to give corresponding heterocoupled products in good to high yields with excellent tolerance towards different functional groups (Table 1.2, entries **44a-d**, **44j**, **44m**, **44n**, **44p-44w**, and **44z-44zb**). Interestingly, substrates with bromo and chloro functional groups also reacted smoothly and gave corresponding heterocoupled products **44w** and **44x** in 60% and 53% yield, respectively.

Heterocycles such as benzimidazole and imidazole which are considered inactivated (higher *pK_a* value) as compare to thiazoles also showed good reactivity towards the CDC reaction with thiophene, benzothiazole and furan (Table 1.2, entries **44a-44l**). No significant electronic effect of substituent on C-2 phenyl ring of imidazopyridine was observed (Table 1.2, entry **44t vs 44u**). The protocol could also be applied for heterocoupling of two different thiophene reaction partners to give heterocoupled product **44y** in 76% yield (Table 1.2, entry **44y**).

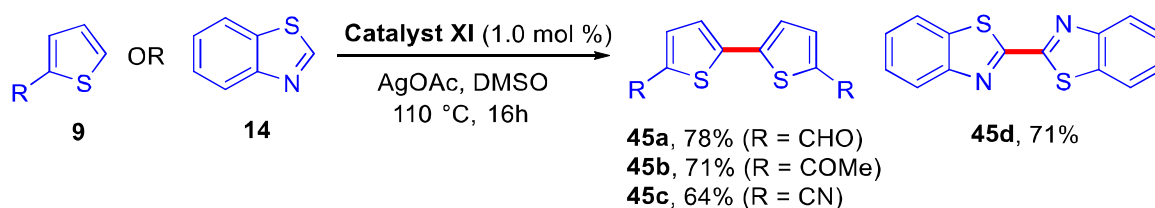
Table 1.2: Substrate scope for the **XI**-catalyzed cross-dehydrogenative heterocoupling reaction^{a,b}

^aReaction conditions: **14** (0.757 mmol), **9** (3.030 mmol), **Catalyst XI** (1.0 mol %), AgOAc (1.5 mmol), DMSO (3 mL), 110 °C, 16 h. ^bIsolated yield.

A comparison of the performance of catalyst **XI** with previously reported literature using palladium catalysts for the CDC of heteroarenes is justified. Most of the earlier reports have used palladium precursors like Pd(OAc)₂, PdBr₂, Pd(TFA)₂ *etc.* as catalyst. Pd(OAc)₂ in 5-10 mol % catalyst loading, KF, AgNO₃, DMF, 120 °C, 24 h³³ or AgNO₃, Phen (30 mol %), DMSO, 110 °C, 10 h³⁴ were used to achieve 11-95% yield of desired products. Instead of Pd(OAc)₂ when Pd(TFA)₂ (5 mol %) with Cu(OAc)₂·H₂O, DMSO, N₂, 8 h was used 25-95% of coupled product was achieved.⁷⁸ Pd(dppf)Cl₂ (2.5 mol %)⁷⁹ and PdBr₂ (10 mol %)³⁵ were also screened as catalyst and both require 120-140 °C reaction temperature, use of external ligand and long reaction time (upto 30 h) to give good conversion (36-95%) of desired product. A halo-bridged abnormal NHC

palladium complex is reported to catalyze the CDC reaction of heteroarenes with 2 mol % catalyst loading to achieve 55-95% yield of desired product.³⁶ As mentioned, earlier reported protocols required higher catalyst loading, longer reaction times, and a substantially higher reaction temperature compared to our standard protocol to achieve good yields. Also, it is worth mentioning here that as compare to literature reports we have tested a broad substrate scope that include all type of (hetero)arens to justify the broad utility of current protocol. The reaction conditions reported in this work are milder compared to other reports in terms of reaction temperature, time, and catalyst loading. It should also be stated that this catalyst functions well without the need for an inert atmosphere.

During the course of reaction optimization formation of homocoupled product **45a** was observed in 21% yield when less amount of **9a** was used (**Table 1.1, entry 14**). This observation made us keen to investigate feasibility of homocoupling reaction using **XI** as catalyst. To our delight, reaction of thiophenes (**9**) or benzothiazole (**14**) using **XI** (1.0 mol %) in the presence of AgOAc (1.5 mmol) in DMSO (3 mL) at 110 °C after 16 h gave corresponding homocoupled products **45a-d** in good (64–78%) yields (**Scheme 1.20**).



Scheme 1.20. Catalytic cross-dehydrogenative homocoupling reaction.

Reusability is one of the most important features of the catalyst both from cost of the process and green chemistry aspects. We thus decided to study reusability of the catalyst **XI** for homocoupling reaction of **9a**. After completion of a fresh reaction cycle (after 16h), another fresh lot of **9a** and AgOAc was added to the reaction vessel and conversion was monitored by ¹H NMR. Interestingly, catalyst **XI** showed excellent activity until four reaction cycles with a little decrease in the conversion percentage in the subsequent cycles (**Figure 1.15**).

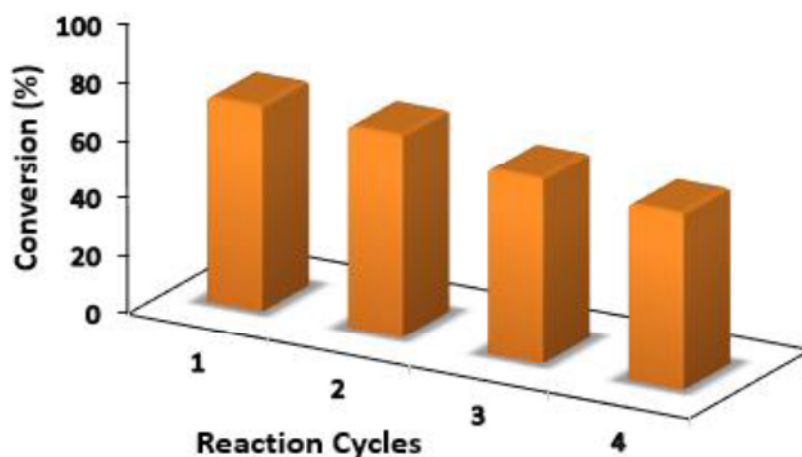
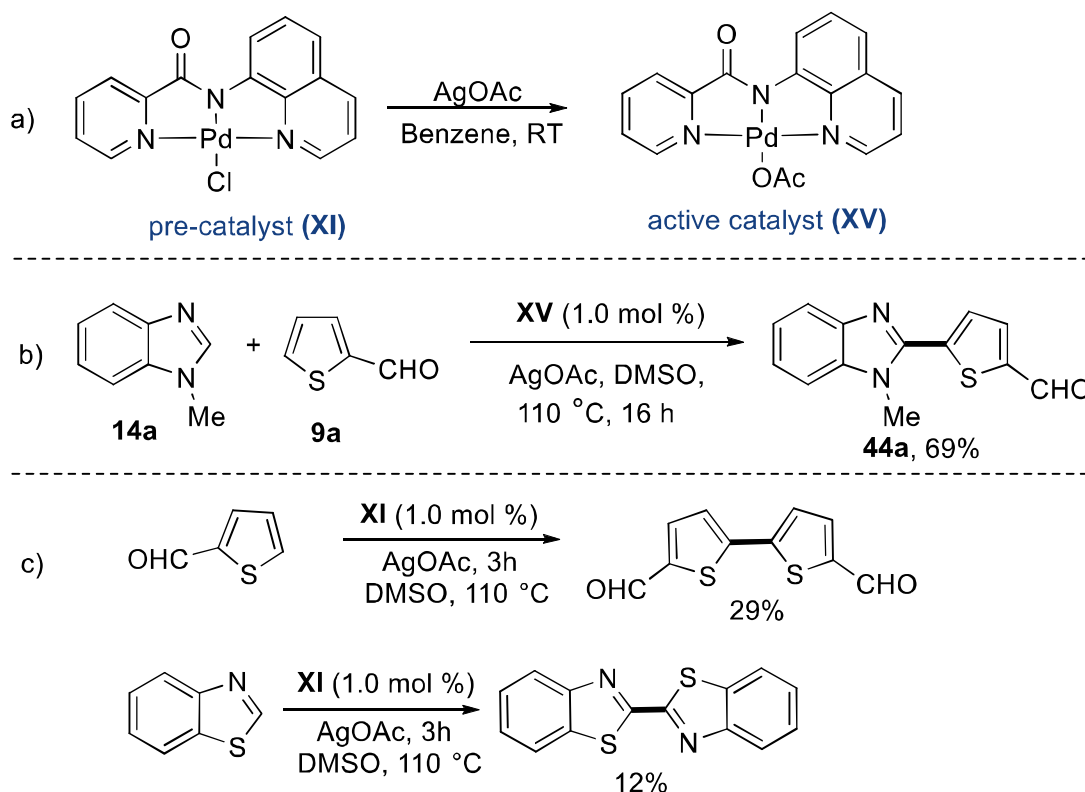


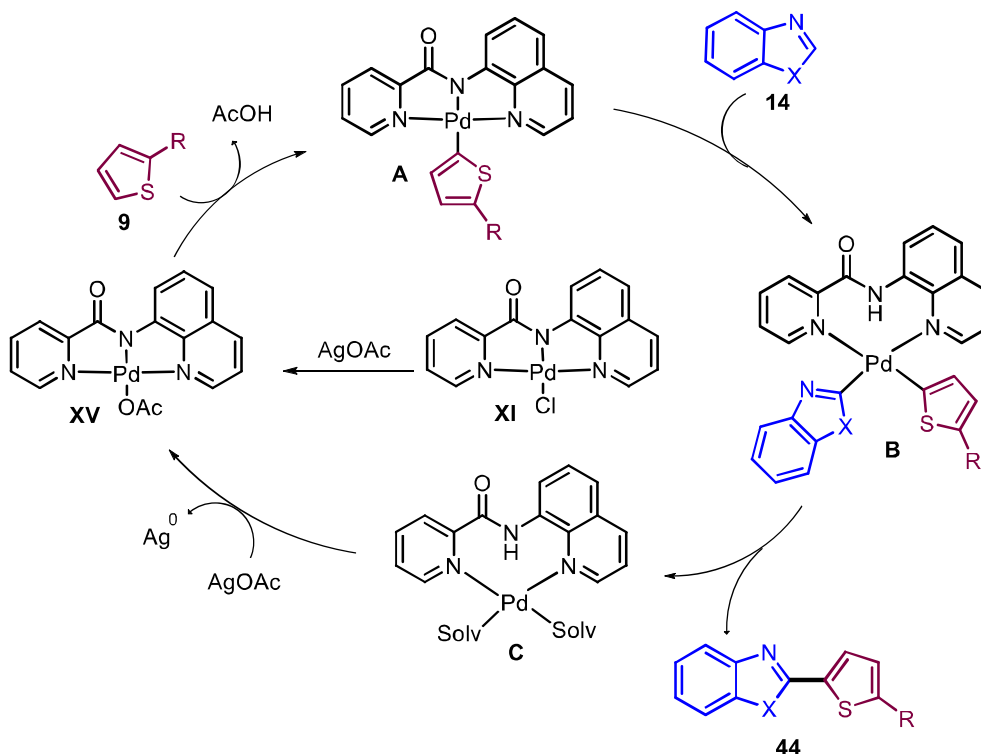
Figure 1.15. Catalytic life of **XI** under optimal conditions

To understand the mechanism of CDC reaction, a series of experiments were performed. First, a stoichiometric reaction of **XI** and AgOAc was performed under an inert atmosphere and observed that the appearance of three new peaks at 1.83, 23.42, and 186.1 ppm in ^1H and $^{13}\text{C}\{^1\text{H}\}$ NMR spectrum of the isolated product (**XV**) suggested replacement of chlorine ligands from acetate group (**Scheme 1.21a**). We then used isolated **XV** as a catalyst for CDC reaction of **14a** with **9a** under standard reaction conditions, and it gave desired coupled product **44a** in 69% yield (**Scheme 1.21b**). This indicates that **XV** is an active catalyst in the reaction and it gets generated *in situ* during the course of catalytic reaction cycle. Further, a reaction of **XI**, AgOAc, and benzothiazole at 110 °C in DMSO- d_6 for 6 h was carried out. In the ^1H NMR of the reaction mixture, the disappearance of C2 peak of benzothiazole was observed indicating abstraction of C2 hydrogen during catalysis. Next, we investigated relative reactivity of benzothiazole and 2-formylthiophene separately in the homocoupling reaction over a period of 3h (**Scheme 1.21c**). Experiments showed 2-formylthiophene is more reactive than benzothiazole as homocoupling of 2-formylthiophene gave 29% of the product, whereas benzothiazole resulted in only 12% of homocoupled product. This result was in agreement with previous reports which mentioned that among *N*-methylbenzimidazole and thiophene, the C2 proton of thiophene is abstracted faster than that of the *N*-methylbenzimidazole.³²



Scheme 1.21. Control experiments.

On the basis of control experiments, a plausible mechanism cycle is proposed for the **XI**-catalyzed CDC of heteroarenes as shown in **Scheme 1.22**. In first step, **XI** upon reaction with AgOAc converts into **XV**, which is termed as catalyst activation step. In next step, **XV** undergoes palladation with more reactive heteroarenes (thiophene) and forms intermediate **A** by releasing one acetic acid molecule. Earlier reports also proposed the formation of ligand-stabilized HetAr-PdL_n intermediated as the catalytic cycle initiation step.³³ Intermediate **A** then promotes the second C–H activation of less reactive heteroarenes (benzothiazole) and forms a *bis*-heteroaryl Pd intermediate (**B**). The *bis*-heteroaryl Pd intermediate (**B**) then upon reductive elimination gives coupled product and solvent ligated Pd(0) species (**C**), which finally upon oxidation with AgOAc regenerates the active catalyst (**XV**).



Scheme 1.22. Plausible mechanism for the **XI**-catalyzed cross-dehydrogenative coupling of heteroarenes.

1.3 CONCLUSION

In summary, we have successfully synthesized a new class of palladium complexes of NNN/CNN pincer ligands. The complexes were characterized with the help of IR, NMR, and HRMS analysis. The structure of complexes and bonding of palladium with ligands was authenticated by single crystal X-ray study. These complexes were found to be very efficient catalyst for the hetero cross dehydrogenative coupling reaction of thiophene, furan and benzothiazole derivatives with a wide range of heteroarenes such as *N*-methylbenzimidazole, *N*-methylimidazole, benzothiazole, and imidazo[1,2-*a*]pyridines and homo cross dehydrogenative coupling reaction of thiophenes and benzothiazoles. The catalyst showed high functional group tolerance and only 1.0 mol % of the catalyst loading is required to achieve good yields in short reaction time. The catalyst can be reused efficiently up to four reaction cycles for the homocoupling of 2-formylthiophene. Mechanism of CDC reaction was proposed on the basis of several control experiments and shown that acetate analog of palladium catalyst (**XV**) is an active catalyst and it generates *in situ* during the catalytic reaction.

1.4 EXPERIMENTAL SECTION

1.4.1 General Materials and Methods

All the reactions were performed in pressure tube under aerobic conditions. HPLC grade hexane, DMSO, DMF, DMA, THF, DCE and NMP were used directly for the reactions. CDCl_3 (Sigma Aldrich), $\text{DMSO-}d_6$ (Sigma Aldrich), silver acetate (Alfa Aesar), $\text{Pd}(\text{OAc})_2$ (Alfa Aesar, 45.9-48.4%), PdCl_2 (Sigma Aldrich, 99.9%), benzothiazole (Alfa Aesar), 1-methyl-1*H*-imidazole (Alfa Aesar), 1-methyl-1*H*-benzimidazole (Alfa Aesar), 2-thiophene carboxaldehyde (Alfa Aesar), 8-aminoquinoline (Sigma Aldrich), 2-picolinic acid (SDFCL), benzoyl chloride (Merck) and others reagents were used as purchased. All other reagents used for CDC reactions were purchased from commercial sources and used as it is. The *N*-(quinolin-8-yl)benzamide⁸⁰, 2-phenylimidazo[1,2-*a*]pyridine⁸¹, *N*-(quinolin-8-yl)picolinamide^{80, 82} were synthesized by reported methods. The derivatives of 2-phenylimidazo[1,2-*a*]pyridine used in CDC reaction were prepared by using literature reported procedure.⁸³ Technical grade solvents for extraction and chromatography (hexane, EtOAc, DCM, Methanol) were used without purification. ^1H , ^{13}C NMR spectra were recorded in CDCl_3 at room temperature on Bruker 400 (400 MHz) spectrometer and FID was processed in NMR topspin software, referenced as follows (δ , ppm): ^1H , residual internal CHCl_3 (7.26); $^{13}\text{C}\{^1\text{H}\}$, internal CDCl_3 (77.00). The following abbreviations were used for NMR spectra to represent the signal multiplicity: singlet (s), broad singlet (br.s), doublet (d), triplet (t), quartet (q), quintet (quint), sextet (sext), septet (sept) and multiplet (m) and their combinations of them as well. The coupling constant (J) and chemical shift (δ) are expressed in Hertz (Hz) and parts per million (ppm) respectively with TMS as internal standard. All the products were purified by column chromatography on silica gel (100-200 mesh). Progress of reaction was monitored by TLC on 0.25 mm silica gel 60-F254. Melting points were recorded using a Stanford Research Systems EZ-Melt automated apparatus. IR spectra were recorded as a neat sample on a Shimadzu IRAffinity-1S spectrometer and values are expressed in cm^{-1} . HRMS measurements were carried out by electrospray ionization (ESI) method on an Agilent Q-TOF LC-MS spectrometer.

1.4.2 Synthesis of Complex XI. A pressure tube was charged with *N*-(quinolin-8-yl) picolinamide (0.050 g, 0.200 mmol), dichloroethane (5 mL) and heated for 1 h at 65 °C. The PdCl₂ (0.036 g, 0.200 mmol) was then added and reaction mixture was heated for 12 h. After 12 h the mixture was cooled to room temperature, solvent was reduced by using rotary evaporator. The remaining mixture was chromatographed on silica gel, using hexane (50 mL) and then EtOAc/hexane (80:20 v/v) to give complex **XI** as a yellow solid (0.070 g, 90%), mp: 328-330 °C. Anal. Calcd (%) for C₁₅H₁₀ClN₃OPd (390.13): C, 46.18; H, 2.58; found C, 46.53; H, 2.29.

NMR (CDCl₃, δ/ppm): ¹H (400 MHz) 8.97 (dd, *J* = 5.1, 1.5 Hz, 1H), 8.90 (dd, *J* = 5.5, 1.5 Hz, 1H), 8.80 (dd, *J* = 7.8, 1.2 Hz, 1H), 8.32 (dd, *J* = 8.3, 1.5 Hz, 1H), 8.06 (td, *J* = 7.7, 1.6 Hz, 1H), 7.97 (dd, *J* = 7.9, 1.8 Hz, 1H), 7.57 (t, *J* = 7.9 Hz, 1H), 7.51 (ddd, *J* = 7.3, 5.4, 1.6 Hz, 1H), 7.46-7.43 (m, 2H); ¹³C{¹H} (100 MHz) δ 166.4, 157.7, 150.0, 149.8, 147.7, 144.9, 140.0, 138.9, 129.9, 129.3, 127.0, 125.7, 121.2, 120.8, 120.8; FT-IR_{vmax} (neat) 3093, 1635, 1573, 1226, 748 cm⁻¹; HRMS (ESI) calcd. for C₁₅H₁₀N₃OPd [M - Cl]⁺: 353.9859, found 353.9845.

1.4.3 Synthesis of Complex XII. *N*-(Quinolin-8-yl)benzamide (0.050 g, 0.201 mmol), 2-phenylimidazo[1,2-*a*]pyridine (0.039 g, 0.201 mmol), dichloroethane (5 mL), and Pd(OAc)₂ (0.135 g, 0.201 mmol) were taken in a pressure tube using procedure same as **XI**. A similar workup gave complex **XII** as a yellow solid (0.096 g, 87%), mp: 234-236 °C. Anal. Calcd (%) for C₂₉H₂₀N₄OPd (546.91): C, 63.69; H, 3.69; found C, 63.84; H, 3.46.

NMR (CDCl₃, δ/ppm): ¹H (400 MHz) 9.24 (dd, *J* = 7.9, 1.2 Hz, 1H), 8.63-8.61 (m, 2H), 8.36 (d, *J* = 9.1 Hz, 1H), 8.26 (d, *J* = 6.8 Hz, 1H), 8.04-8.01 (m, 2H), 7.59 (dd, *J* = 7.5, 1.6 Hz, 1H), 7.52 (t, *J* = 8.0 Hz, 1H), 7.46 (dd, *J* = 4.7, 1.6 Hz, 1H), 7.33-7.27 (m, 3H), 7.23-7.19 (m, 2H), 7.06-7.02 (m, 1H), 7.00-7.97 (m, 2H), 6.83 (td, *J* = 7.3, 1.5 Hz, 1H), 6.32 (d, *J* = 6.7 Hz, 1H); ¹³C{¹H} (100 MHz) δ 177.9, 148.9, 148.8, 148.2, 146.0, 145.5, 145.3, 145.2, 137.7, 132.4, 131.0, 130.1, 129.4, 129.3, 129.2, 128.9, 127.6, 127.5, 127.2, 126.0, 124.1, 120.3, 120.0, 119.1, 117.5, 114.6, 110.3; FT-IR_{vmax} (neat) 3078, 1604, 1566, 1234, 740 cm⁻¹; HRMS (ESI) calcd for C₂₉H₂₁N₄OPd [M + H]⁺: 547.0745, found 547.0742.

1.4.4 Synthesis of Complex XIII. *N*-(Quinolin-8-yl)benzamide (0.050 g, 0.201 mmol) and benzothiazole (0.027 g, 0.201 mmol), dichloroethane (5 mL), and Pd(OAc)₂ (0.135 g, 0.201 mmol) were taken in a pressure tube using procedure same as complex **XI**. A similar workup gave complex **XIII** as a yellow solid (0.091 g, 93%), mp: 152-154 °C. Anal. Calcd (%) for C₂₃H₁₅N₃OPdS (487.87): C, 56.62; H, 3.10; found C, 59.18; H, 2.97.

NMR (CDCl₃, δ/ppm): ¹H (400 MHz) 9.68 (s, 1H), 9.08 (dd, *J* = 8.0, 1.1 Hz, 1H), 8.75 (dd, *J* = 8.1, 1.4 Hz, 1H), 8.05-8.03 (m, 1H), 7.94 (dd, *J* = 8.3, 1.5 Hz, 1H), 7.61-7.54 (m, 3H), 7.45-7.39 (m, 2H), 7.11 (dd, *J* = 8.1, 1.2 Hz, 1H), 7.07 (td, *J* = 7.4, 1.2 Hz, 1H), 6.99 (dd, *J* = 8.3, 4.7 Hz, 1H), 6.83 (td, *J* = 7.3, 1.6 Hz, 1H), 6.12 (dd, *J* = 7.4, 1.2 Hz, 1H); ¹³C{¹H} (100 MHz) δ 177.4, 158.6, 150.4, 148.7, 148.5, 147.4, 145.5, 145.4, 137.8, 131.9, 131.9, 129.9, 129.7, 129.3, 127.9, 127.7, 127.4, 124.6, 124.6, 122.5, 120.6, 120.1, 117.9; FT-IR_{v_{max}} (neat) 3039, 1604, 1566, 1265, 756 cm⁻¹; HRMS (ESI) calcd for C₁₆H₁₀KN₂OPd [M – L4 + H]⁺: 352.9906, found 352.9903.

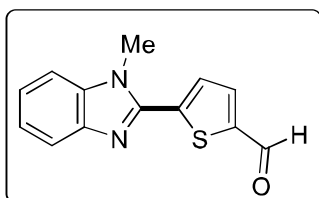
1.4.5 Synthesis of Complex XIV. *N*-(Quinolin-8-yl)benzamide (0.050 g, 0.201 mmol), *N*-methyl imidazole (0.016 g, 0.201 mmol), dichloroethane (5 mL) and Pd(OAc)₂ (0.135 g, 0.201 mmol) were taken in a pressure tube using procedure same as **XI**. A similar workup gave complex **XIV** as a yellow solid (0.075 g, 86%), mp: 140-142 °C. Anal. Calcd (%) for C₂₀H₁₆N₄OPd (434.78): C, 55.25; H, 3.71; found C, 55.11; H, 3.57.

NMR (CDCl₃, δ/ppm): ¹H (400 MHz) δ 9.02 (d, *J* = 7.9 Hz, 1H), 8.22 (s, 1H), 7.71 (d, *J* = 8.3 Hz, 1H), 7.57-7.54 (m, 2H), 7.40 (t, *J* = 7.9 Hz, 1H), 7.10-6.93 (m, 5H), 6.83-6.82 (m, 1H), 6.51 (d, *J* = 7.3 Hz, 1H), 3.46 (s, 3H); ¹³C{¹H} (100 MHz) δ 177.4, 149.7, 149.0, 147.4, 145.5, 145.1, 139.4, 137.1, 132.1, 130.5, 129.6, 128.9, 128.9, 127.6, 124.3, 121.3, 120.5, 119.8, 117.8, 34.3; FT-IR_{v_{max}} (neat) 3039, 1604, 1538, 1234, 732 cm⁻¹; HRMS (ESI) calcd for C₁₆H₁₀KN₂OPd [M – L5 + K]⁺: 390.9465, found 391.4953.

1.4.6 Synthesis of Complex XV. A pressure tube was combined with complex **XI** (0.050 g, 0.128 mmol), AgOAc (0.021 g, 0.128 mmol), benzene (5 mL) and allowed to stir at room temperature for 12 h under nitrogen atmosphere. The solvent was reduced by using rotary evaporated. The remaining mixture was chromatographed on silica gel, eluted with DCM (50 mL) and then MeOH/DCM (10:90 v/v) to give complex **XV** as a yellow solid (0.037 g, 70%), mp: 295-297 °C. **NMR** (CDCl₃, δ/ppm): ¹H (400 MHz) δ 8.99 (dd, *J* = 5.1, 1.5 Hz, 1H), 8.91 (dd, *J* = 5.5, 1.5 Hz, 1H), 8.82 (dd, *J* = 7.8, 1.1 Hz, 1H), 8.33 (dd, *J* = 8.3, 1.5 Hz, 1H), 8.06 (td, *J* = 7.7, 1.6 Hz, 1H), 7.97 (dd, *J* = 7.8, 1.6 Hz, 1H), 7.58 (t, *J* = 7.9 Hz, 1H), 7.52 (ddd, *J* = 7.3, 5.4, 1.6 Hz, 1H), 7.48-7.44 (m, 2H), 1.83 (s, 3H, COCH₃); ¹³C{¹H} (100 MHz) δ 186.1 (-C=O), 166.7, 158.0, 150.4, 150.1, 148.0, 145.2, 140.3, 139.2, 130.3, 129.7, 127.3, 126.0, 125.0, 121.5, 121.2, 23.4 (COCH₃); FT-IR _{v_{max}} (neat) 2954, 1735, 1639, 1573, 1257 cm⁻¹.

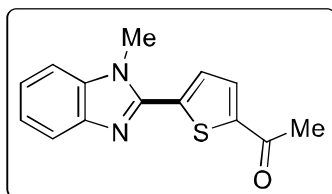
1.4.7 General Procedure for Hetero Cross Dehydrogenative Coupling. A pressure tube (10 mL) was charged with heteroarene (**14**, 0.757 mmol), heteroarene (**9**, 3.030 mmol), AgOAc (1.500 mmol), catalyst **XI-XIV** (1.0 mol %) and DMSO (3 mL). The reaction mixture was then stirred for 16 h, on 110 °C temp of oil bath. Progress of reaction was monitored with the help of TLC to achieve the maximum conversion of coupled product. After attaining the maximum conversion, reaction was stopped and mixture was cooled to room temperature and water (15 mL) was added to reaction mixture. The extract was then washed with ethyl acetate (20 mL): water (15 mL) and dried with anhydrous Na₂SO₄. The solvent was then removed using rotary evaporator and mixture was chromatographed on silica column (1 × 15 cm), using appropriate ratio of ethyl acetate and hexane to give final coupled products.

5-(1-Methyl-1H-benzo[d]imidazol-2-yl)thiophene-2-carbaldehyde (44a): Yellow solid; mp:



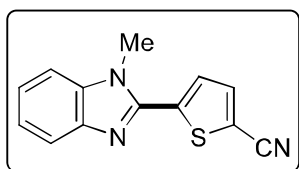
130-132 °C; (Lit⁸⁴. mp: 135-137 °C); ¹H NMR (400 MHz, CDCl₃) δ 9.93 (s, 1H), 7.81–7.79 (m, 1H), 7.78 (d, *J* = 3.9 Hz, 1H), 7.69 (d, *J* = 4.0 Hz, 1H), 7.37–7.29 (m, 3H), 3.99 (s, 3H); ¹³C{¹H} NMR (100 MHz, CDCl₃) δ 182.7, 146.1, 144.8, 142.5, 140.8, 136.6, 136.1, 128.6, 123.9, 123.2, 120.0, 109.7, 31.8.

1-(5-(1-Methyl-1H-benzo[d]imidazol-2-yl)thiophen-2-yl)ethan-1-one (44b): Yellow solid; mp:



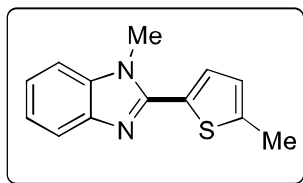
170-172 °C; ¹H NMR (400 MHz, CDCl₃) δ 7.83–7.81 (m, 1H), 7.72 (s, 2H), 7.39–7.36 (m, 1H), 7.35–7.30 (m, 2H), 4.02 (s, 3H), 2.60 (s, 3H); ¹³C{¹H} NMR (100 MHz, CDCl₃) δ 190.5, 146.3, 145.9, 142.0, 138.7, 136.4, 132.4, 129.3, 123.9, 123.4, 119.8, 109.7, 31.9, 27.0.

5-(1-Methyl-1H-benzo[d]imidazol-2-yl)thiophene-2-carbonitrile (44c)⁸⁵: Yellow solid; mp:



170-172 °C; ¹H NMR (400 MHz, CDCl₃) δ 7.84–7.77 (m, 1H), 7.67 (d, *J* = 4.0 Hz, 1H), 7.52 (d, *J* = 4.0 Hz, 1H), 7.40–7.31 (m, 3H), 4.01 (s, 3H); ¹³C{¹H} NMR (100 MHz, CDCl₃) δ 145.2, 142.6, 139.7, 137.8, 136.6, 126.8, 124.1, 123.3, 120.2, 113.6, 111.7, 109.7, 31.8.

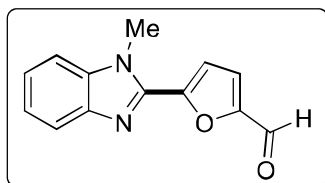
1-Methyl-2-(5-methylthiophen-2-yl)-1H-benzo[d]imidazole (44d)⁸⁶: White solid; mp: 78-80



°C; ¹H NMR (400 MHz, CDCl₃) δ 7.79–7.77 (m, 1H), 7.36 (d, *J* = 3.7 Hz, 1H), 7.31–7.34 (m, 1H), 7.30–7.26 (m, 2H), 6.84–6.83 (m, 1H), 3.94 (s, 3H), 2.56 (s, 3H); ¹³C{¹H} NMR (100 MHz, CDCl₃) δ 148.1, 143.5, 142.9, 136.5, 130.0, 128.0, 126.1, 122.6, 122.4, 119.5, 109.2,

31.6, 15.4.

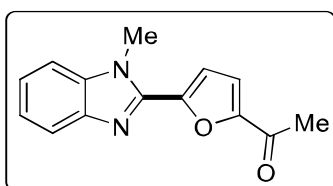
5-(1-Methyl-1H-benzo[d]imidazol-2-yl)furan-2-carbaldehyde (44e): Yellow solid; mp: 135-



138 °C; (Lit.⁸⁴ mp: 139-142 °C); ¹H NMR (400 MHz, CDCl₃) δ 9.74 (s, 1H), 7.82 (d, *J* = 7.2 Hz, 1H), 7.50 (d, *J* = 3.8 Hz, 1H), 7.44–7.32 (m, 4H), 4.17 (s, 3H); ¹³C{¹H} NMR (100 MHz, CDCl₃) δ 177.2, 152.9, 149.9, 142.1, 136.0, 124.4, 123.6, 122.5, 119.8, 114.7, 109.9,

32.0.

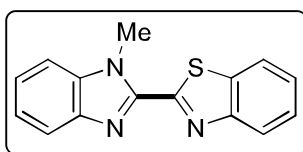
1-(5-(1-Methyl-1H-benzo[d]imidazol-2-yl)furan-2-yl)ethan-1-one (44f): Yellow solid; mp:



138-140 °C; ¹H NMR (400 MHz, CDCl₃) δ 7.81 (dd, *J* = 7.2, 1.3 Hz, 1H), 7.44–7.42 (m, 1H), 7.38 (dd, *J* = 7.0, 1.2 Hz, 1H), 7.39–7.31 (m, 3H), 4.17 (s, 3H), 2.58 (s, 3H); ¹³C{¹H} NMR (100 MHz, CDCl₃) δ 186.0, 152.8, 149.1, 142.9, 142.8, 136.3, 123.9, 123.2,

120.1, 118.9, 114.0, 109.7, 31.9, 26.2.

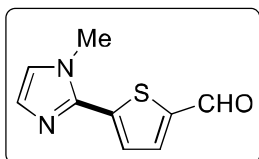
2-(1-Methyl-1H-benzo[d]imidazol-2-yl)benzo[d]thiazole (44g)⁸⁷: White solid; mp: 217-219 °C;



¹H NMR (400 MHz, CDCl₃) δ 8.11 (d, *J* = 8.0 Hz, 1H), 7.98–7.96 (m, 1H), 7.88 (d, *J* = 8.1 Hz, 1H), 7.55–7.50 (m, 1H), 7.47–7.43 (m, 2H), 7.471–7.32 (m, 2H), 4.42 (s, 3H); ¹³C{¹H} NMR (100 MHz, CDCl₃)

δ 159.8, 154.0, 145.2, 142.7, 137.2, 135.3, 126.4, 126.1, 124.4, 123.8, 123.2, 121.7, 120.5, 110.1, 32.3; HRMS (ESI) calcd for C₁₅H₁₂N₃S [M+H]⁺: 266.0746, found 266.0735.

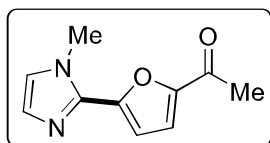
5-(1-Methyl-1H-imidazol-2-yl)thiophene-2-carbaldehyde (44h): Yellow solid; mp: 106-108



°C; (Lit.⁸⁴ mp: 105-108 °C); ¹H NMR (400 MHz, CDCl₃) δ 9.93 (s, 1H), 7.77 (d, *J* = 4.0 Hz, 1H), 7.54 (d, *J* = 4.0 Hz, 1H), 7.18 (s, 1H), 7.02 (s, 1H), 3.92 (s, 3H); ¹³C{¹H} NMR (100 MHz, CDCl₃) δ 182.8, 143.4, 141.1,

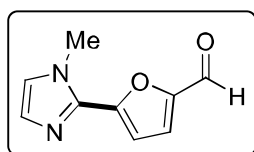
136.5, 129.2, 126.7, 124.1, 35.1.

1-(5-(1-Methyl-1*H*-imidazol-2-yl)thiophen-2-yl)ethan-1-one (44i): Yellow solid; mp: 126-128



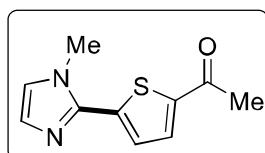
°C; ^1H NMR (400 MHz, CDCl_3) δ 7.68 (d, $J = 4.0$ Hz, 1H), 7.50 (d, $J = 4.0$ Hz, 1H), 7.14 (d, $J = 0.8$ Hz, 1H), 6.99 (d, $J = 0.8$ Hz, 1H), 3.89 (s, 3H), 2.57 (s, 3H); $^{13}\text{C}\{^1\text{H}\}$ NMR (100 MHz, CDCl_3) δ 190.6, 144.1, 141.2, 139.6, 132.7, 128.8, 126.9, 123.8, 35.1, 26.9.

5-(1-Methyl-1*H*-imidazol-2-yl)furan-2-carbaldehyde (44j): Yellow solid; mp: 73-75 °C; ^1H



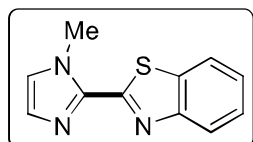
NMR (400 MHz, CDCl_3) δ 9.65 (s, 1H), 7.34 (d, $J = 3.7$ Hz, 1H), 7.25 (d, $J = 3.8$ Hz, 1H), 7.18 (s, 1H), 7.01 (s, 1H), 4.04 (s, 3H); $^{13}\text{C}\{^1\text{H}\}$ NMR (100 MHz, CDCl_3) δ 176.9, 152.1, 150.2, 137.3, 128.9, 124.0, 123.2, 111.9, 35.5.

1-(5-(1-Methyl-1*H*-imidazol-2-yl)furan-2-yl)ethan-1-one (44k): Yellow solid; mp: 115-117 °C;



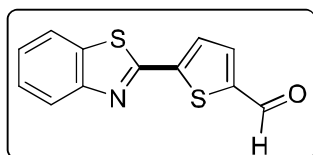
^1H NMR (400 MHz, CDCl_3) δ 7.28 (d, $J = 3.8$ Hz, 1H), 7.15 (s, 1H), 7.04 (d, $J = 3.7$ Hz, 1H), 6.97 (s, 1H), 4.02 (s, 3H), 2.52 (s, 3H); $^{13}\text{C}\{^1\text{H}\}$ NMR (100 MHz, CDCl_3) δ 185.9, 151.9, 149.4, 138.0, 129.5, 123.6, 119.2, 111.0, 35.2, 26.1.

2-(1-Methyl-1*H*-imidazol-2-yl)benzo[*d*]thiazole (44l): Pale yellow solid; mp: 137-139 °C;



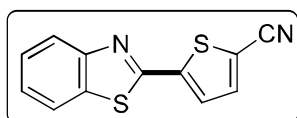
(Lit.³³ mp: 134-136 °C); ^1H NMR (400 MHz, CDCl_3) δ 8.02–8.00 (m, 1H), 7.93–7.91 (m, 1H), 7.50–7.45 (m, 1H), 7.41–7.37 (m, 1H), 7.19 (d, $J = 1.0$ Hz, 1H), 7.06 (s, 1H), 4.25 (s, 3H); $^{13}\text{C}\{^1\text{H}\}$ NMR (100 MHz, CDCl_3) δ 159.6, 154.0, 140.6, 134.8, 129.7, 126.1, 125.4, 125.0, 123.2, 121.6, 35.7.

5-(Benzo[*d*]thiazol-2-yl)thiophene-2-carbaldehyde (44m): Yellow solid; mp: 147-149 °C;



(Lit.³⁴ mp: 146-148 °C); ^1H NMR (400 MHz, CDCl_3) δ 9.97 (s, 1H), 8.10–8.07 (m, 1H), 7.94–7.86 (m, 1H), 7.78 (d, $J = 4.0$ Hz, 1H), 7.72 (d, $J = 4.0$ Hz, 1H), 7.55–7.50 (m, 1H), 7.45–7.41 (m, 1H); $^{13}\text{C}\{^1\text{H}\}$ NMR (100 MHz, CDCl_3) δ 182.9, 159.7, 153.6, 145.6, 145.2, 136.2, 135.2, 128.4, 126.9, 126.2, 123.7, 121.6.

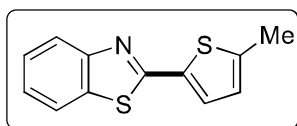
5-(Benzo[*d*]thiazol-2-yl)thiophene-2-carbonitrile (44n): Pale green solid; mp: 169-171 °C;



(Lit.³⁴ mp: 176-178 °C); ^1H NMR (400 MHz, CDCl_3) δ 8.07 (d, $J = 8.1$ Hz, 1H), 7.90 (d, $J = 7.8$ Hz, 1H), 7.63–7.57 (m, 2H), 7.55–7.51 (m,

1H), 7.46–7.42 (m, 1H); $^{13}\text{C}\{^1\text{H}\}$ NMR (100 MHz, CDCl_3) δ 158.7, 153.4, 143.8, 137.9, 135.0, 127.5, 127.0, 126.3, 123.6, 121.7, 113.7, 112.1.

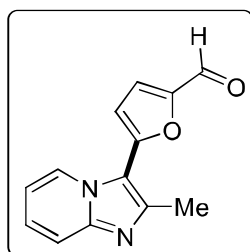
2-(5-Methylthiophen-2-yl)benzo[d]thiazole (44o): Yellow solid; mp: 98–100 °C; (Lit.³⁴ mp: 95–



97 °C); ^1H NMR (400 MHz, CDCl_3) δ 8.00 (d, $J = 8.1$ Hz, 1H), 7.81–7.81 (m, 1H), 7.47–7.43 (m, 2H), 7.36–7.32 (m, 1H), 6.80 (dd, $J = 3.7$, 1.1 Hz, 1H), 2.56 (s, 3H); $^{13}\text{C}\{^1\text{H}\}$ NMR (100 MHz, CDCl_3) δ 161.6,

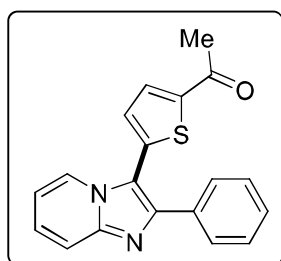
153.7, 144.7, 134.8, 134.5, 128.9, 126.4, 126.3, 124.9, 122.7, 121.4, 15.7.

5-(2-Methylimidazo[1,2-a]pyridin-3-yl)furan-2-carbaldehyde (44p): Pale red solid; mp: 145–



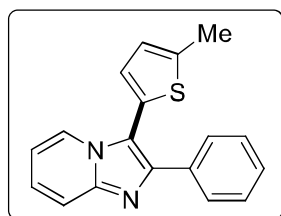
147 °C; ^1H NMR (400 MHz, CDCl_3) δ 9.64 (s, 1H), 8.95 (dt, $J = 7.0$, 1.2 Hz, 1H), 7.62 (dt, $J = 8.9$, 1.2 Hz, 1H), 7.42 (d, $J = 3.8$ Hz, 1H), 7.33–7.29 (m, 1H), 6.98 (td, $J = 6.9$, 1.3 Hz, 1H), 6.70 (d, $J = 3.8$ Hz, 1H), 2.66 (s, 3H); $^{13}\text{C}\{^1\text{H}\}$ NMR (100 MHz, CDCl_3) δ 176.0, 151.7, 150.8, 146.0, 145.7, 126.2, 126.0, 117.1, 113.7, 112.7, 108.3, 15.8; HRMS (ESI) calcd for $\text{C}_{13}\text{H}_{11}\text{N}_2\text{O}_2$ $[\text{M}+\text{H}]^+$: 227.0815, found 227.0815.

1-(5-(2-Phenylimidazo[1,2-a]pyridin-3-yl)thiophen-2-yl)ethan-1-one (44q): Pale green solid;



mp: 135–137 °C; ^1H NMR (400 MHz, CDCl_3) δ 8.16 (d, $J = 6.9$ Hz, 1H), 7.76 (d, $J = 3.8$ Hz, 1H), 7.70–7.68 (m, 3H), 7.37–7.28 (m, 4H), 7.19 (d, $J = 3.8$ Hz, 1H), 6.87 (t, $J = 6.7$ Hz, 1H), 2.61 (s, 3H); $^{13}\text{C}\{^1\text{H}\}$ NMR (100 MHz, CDCl_3) δ 190.4, 145.9, 145.8, 145.5, 138.5, 133.4, 133.0, 130.6, 128.5, 128.4, 128.2, 125.7, 123.7, 117.7, 113.1, 112.9, 26.8; HRMS (ESI) calcd for $\text{C}_{19}\text{H}_{15}\text{N}_2\text{OS}$ $[\text{M}+\text{H}]^+$: 319.0900, found 319.0897.

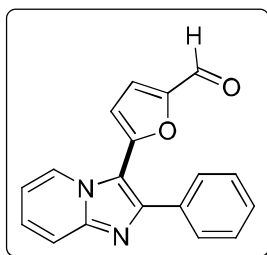
3-(5-Methylthiophen-2-yl)-2-phenylimidazo[1,2-a]pyridine (44r): Pale yellow solid; mp: 109–



111 °C; ^1H NMR (400 MHz, CDCl_3) δ 8.01 (dt, $J = 6.9$, 1.2 Hz, 1H), 7.82–7.79 (m, 2H), 7.66 (d, $J = 9.2$ Hz, 1H), 7.35–7.32 (m, 2H), 7.30–7.26 (m, 1H), 7.24–7.19 (m, 1H), 6.99 (d, $J = 3.6$ Hz, 1H), 6.88–6.87 (m, 1H), 6.79–6.75 (m, 1H), 2.57 (s, 3H); $^{13}\text{C}\{^1\text{H}\}$ NMR (100 MHz, CDCl_3) δ 145.1, 144.2, 143.5, 133.9, 130.5, 128.2, 127.9, 127.7, 127.3, 126.2,

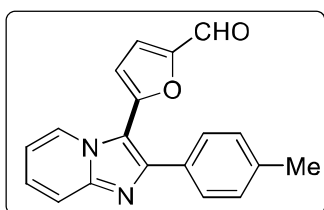
125.0, 123.9, 117.3, 113.9, 112.4, 15.6; HRMS (ESI) calcd for $\text{C}_{18}\text{H}_{15}\text{N}_2\text{S}$ $[\text{M}+\text{H}]^+$: 291.0950, found 291.0948.

5-(2-Phenylimidazo[1,2-*a*]pyridin-3-yl)furan-2-carbaldehyde (44s): Yellow solid; mp: 142-144 °C;



^1H NMR (400 MHz, CDCl_3) δ 9.64 (s, 1H), 8.87 (d, $J = 7.1$ Hz, 1H), 7.72–7.69 (m, 3H), 7.46–7.41 (m, 3H), 7.38–7.33 (m, 1H), 7.29 (d, $J = 3.8$ Hz, 1H), 6.99 (td, $J = 6.9, 1.3$ Hz, 1H), 6.52 (d, $J = 3.8$ Hz, 1H); $^{13}\text{C}\{^1\text{H}\}$ NMR (100 MHz, CDCl_3) δ 176.3, 151.5, 151.1, 148.0, 146.2, 133.7, 128.9, 128.9, 128.6, 126.7, 126.0, 123.5, 117.8, 114.0, 111.6, 110.8; HRMS (ESI) calcd for $\text{C}_{18}\text{H}_{13}\text{N}_2\text{O}_2$ $[\text{M}+\text{H}]^+$: 289.0972, found 289.0959.

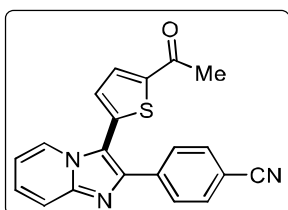
5-(2-(*p*-Tolyl)imidazo[1,2-*a*]pyridin-3-yl)furan-2-carbaldehyde (44t): Pale brown solid; mp:



132-134 °C; ^1H NMR (400 MHz, CDCl_3) δ 9.64 (s, 1H), 8.87 (d, $J = 6.8$ Hz, 1H), 7.71 (d, $J = 9.2$ Hz, 1H), 7.60 (d, $J = 7.6$ Hz, 2H), 7.37–7.33 (m, 1H), 7.29 (d, $J = 3.6$ Hz, 1H), 7.25 (d, $J = 8.0$ Hz, 2H), 7.00–6.97 (m, 1H), 6.54 (d, $J = 4.0$ Hz, 1H), 2.41 (s, 3H); $^{13}\text{C}\{^1\text{H}\}$ NMR (100 MHz, CDCl_3) δ 176.3, 151.4, 148.2, 146.2, 138.8, 130.8, 129.3,

128.8, 126.6, 126.0, 117.7, 113.9, 111.4, 110.7, 21.4; HRMS (ESI) calcd for $\text{C}_{19}\text{H}_{15}\text{N}_2\text{O}_2$ $[\text{M}+\text{H}]^+$: 303.1128, found 303.1117.

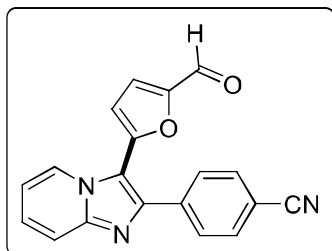
4-(3-(5-Acetylthiophen-2-yl)imidazo[1,2-*a*]pyridin-2-yl)benzotrile (44u): Yellow solid; mp:



200-202 °C; ^1H NMR (400 MHz, CDCl_3) δ 8.09 (dt, $J = 7.0, 1.2$ Hz, 1H), 7.82–7.79 (m, 3H), 7.69 (dt, $J = 9.2, 1.2$ Hz, 1H), 7.61–7.59 (m, 2H), 7.33–7.29 (m, 1H), 7.21 (d, $J = 3.8$ Hz, 1H), 6.89 (td, $J = 6.9, 1.2$ Hz, 1H), 2.63 (s, 3H); $^{13}\text{C}\{^1\text{H}\}$ NMR (100 MHz, CDCl_3) δ 190.3, 146.9, 145.9, 143.0, 138.0, 137.2, 133.0, 132.2, 131.1, 128.5, 126.4, 123.8,

118.8, 117.9, 113.9, 113.6, 111.4, 26.8; HRMS (ESI) calcd for $\text{C}_{20}\text{H}_{14}\text{N}_3\text{OS}$ $[\text{M}+\text{H}]^+$: 344.0852, found 344.0850.

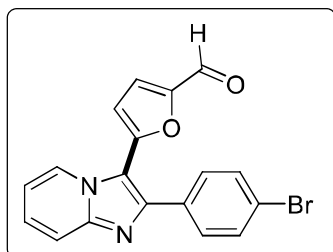
4-(3-(5-Formylfuran-2-yl)imidazo[1,2-*a*]pyridin-2-yl)benzotrile (44v): Yellow solid; mp:



241-243 °C; ^1H NMR (400 MHz, CDCl_3) δ 9.70 (s, 1H), 8.71 (dt, $J = 6.9, 1.2$ Hz, 1H), 7.88–7.86 (m, 2H), 7.73–7.71 (m, 3H), 7.42–7.38 (m, 1H), 7.36 (d, $J = 3.8$ Hz, 1H), 7.02 (td, $J = 6.9, 1.2$ Hz, 1H), 6.60 (d, $J = 3.8$ Hz, 1H); $^{13}\text{C}\{^1\text{H}\}$ NMR (100 MHz, CDCl_3) δ 176.7, 152.1, 149.6, 146.4, 145.2, 138.3, 132.4, 129.3, 128.5, 127.3, 125.7, 123.0,

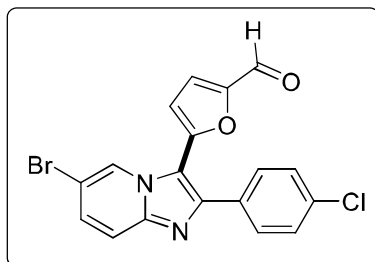
118.7, 118.0, 114.4, 112.3, 112.0; HRMS (ESI) calcd for $C_{19}H_{12}N_3O_2$ $[M+H]^+$: 314.0924, found 314.0917.

5-(2-(4-Bromophenyl)imidazo[1,2-*a*]pyridin-3-yl)furan-2-carbaldehyde (44w): Yellow solid;



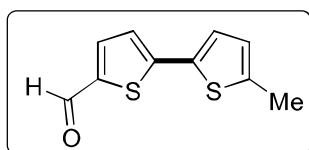
mp: 192-194 °C; 1H NMR (400 MHz, $CDCl_3$) δ 9.67 (s, 1H), 8.80 (dt, $J = 7.0, 1.1$ Hz, 1H), 7.71 (dt, $J = 9.1, 1.1$ Hz, 1H), 7.62–7.57 (m, 4H), 7.39–7.35 (m, 1H), 7.31 (d, $J = 3.8$ Hz, 1H), 7.00 (td, $J = 6.9, 1.3$ Hz, 1H), 6.55 (d, $J = 3.8$ Hz, 1H); $^{13}C\{^1H\}$ NMR (100 MHz, $CDCl_3$) δ 176.5, 151.8, 150.6, 146.6, 146.3, 132.7, 131.9, 130.5, 126.9, 125.9, 123.2, 117.8, 114.1, 111.5, 111.2; HRMS (ESI) calcd for $C_{18}H_{12}BrN_2O_2$ $[M+H]^+$: 367.0077, found 367.0122 and 369.0103.

5-(6-Bromo-2-(4-chlorophenyl)imidazo[1,2-*a*]pyridin-3-yl)furan-2-carbaldehyde (44x); Pale



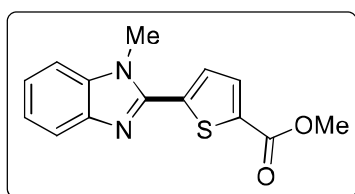
yellow solid; mp: 175-178 °C; 1H NMR (400 MHz, $CDCl_3$) δ 9.83 (s, 1H), 7.97 (s, 1H), 7.86 (dt, $J = 9.1, 2.4$ Hz, 2H), 7.59 (d, $J = 9.5$ Hz, 1H), 7.50 (d, $J = 3.8$ Hz, 1H), 7.44 (d, $J = 9.5$ Hz, 1H), 7.41–7.37 (m, 2H), 7.25 (s, 1H); $^{13}C\{^1H\}$ NMR (100 MHz, $CDCl_3$) δ 177.7, 152.8, 149.4, 145.9, 144.7, 134.3, 131.5, 129.2, 129.0, 127.4, 125.2, 120.8, 119.2, 117.1, 110.4, 109.1; HRMS (ESI) calcd for $C_{18}H_{11}BrClN_2O_2$ $[M+H]^+$: 400.9687, found 400.9674 and 402.9652.

5'-Methyl-[2,2'-bithiophene]-5-carbaldehyde (44y): Yellow solid; mp: 95-97 °C; 1H NMR (400



MHz, $CDCl_3$) δ 9.84 (s, 1H), 7.65 (d, $J = 4.0$ Hz, 1H), 7.16 (t, $J = 4.0$ Hz, 2H), 6.74–6.72 (m, 2H), 2.51 (s, 3H); $^{13}C\{^1H\}$ NMR (100 MHz, $CDCl_3$) δ 182.5, 147.8, 142.4, 141.0, 137.5, 133.7, 126.6, 126.2, 123.4, 15.5; HRMS (ESI) calcd for $C_{10}H_9OS_2$ $[M+H]^+$: 209.0089, found 209.0086.

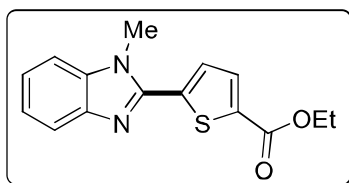
Methyl 5-(1-methyl-1*H*-benzo[*d*]imidazol-2-yl)thiophene-2-carboxylate (44z)²¹: White solid;



mp: 138-140 °C; 1H NMR (400 MHz, $CDCl_3$) δ 7.88 (d, $J = 4.0$ Hz, 1H), 7.84 (dd, $J = 6.8, 2.0$ Hz, 1H), 7.62 (d, $J = 4.0$ Hz, 1H), 7.43–7.34 (m, 3H), 4.04 (s, 3H), 3.96 (s, 3H); $^{13}C\{^1H\}$ NMR (100 MHz, $CDCl_3$) δ 162.3, 146.7, 142.9, 138.6, 136.7, 135.4, 133.6,

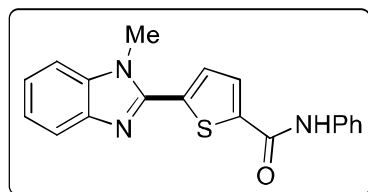
128.1, 123.6, 123.0, 120.1, 109.6, 52.4, 31.8.

Ethyl 5-(1-methyl-1*H*-benzo[*d*]imidazol-2-yl)thiophene-2-carboxylate (44za)²¹: White solid;



mp: 110-112 °C; ¹H NMR (400 MHz, CDCl₃) δ 7.87 (d, *J* = 3.9 Hz, 1H), 7.85 – 7.83 (m, 1H), 7.61 (d, *J* = 4.0 Hz, 1H), 7.43 – 7.32 (m, 3H), 4.42 (q, *J* = 7.1 Hz, 2H), 4.05 (s, 3H), 1.43 (t, *J* = 7.1 Hz, 3H); ¹³C{¹H} NMR (100 MHz, CDCl₃) δ 161.8, 146.6, 142.8, 138.4, 136.7, 135.9, 133.4, 128.0, 123.8, 123.0, 120.1, 109.6, 61.5, 31.8, 14.3.

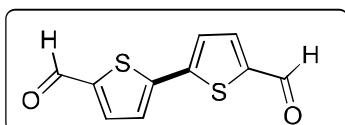
5-(1-Methyl-1*H*-benzo[*d*]imidazol-2-yl)-*N*-phenylthiophene-2-carboxamide (44zb): White



solid; mp: 268-270 °C; ¹H NMR (400 MHz, DMSO-*d*₆) δ 10.38 (s, 1H), 8.14 (d, *J* = 4.0 Hz, 1H), 7.89 (d, *J* = 4.1 Hz, 1H), 7.77 (d, *J* = 7.5 Hz, 2H), 7.68 (t, *J* = 8.6 Hz, 2H), 7.39 (t, *J* = 7.9 Hz, 2H), 7.35 – 7.31 (m, 1H), 7.39 – 7.26 (m, 1H), 7.14 (t, *J* = 7.3 Hz, 1H), 4.08 (s, 3H); ¹³C{¹H} NMR (100 MHz, DMSO-*d*₆) δ 159.9, 146.9, 142.7, 142.2, 139.0, 137.6, 137.2, 130.2, 129.2, 129.0, 124.5, 123.5, 122.9, 120.9, 119.5, 111.1, 32.3.

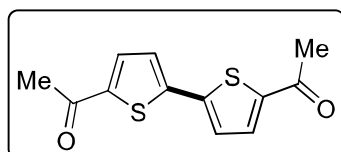
1.4.8 General Procedure for Homo Cross-Dehydrogenative Coupling. DMSO (3 mL), heteroarene (**14/9**, 1.00 mmol), AgOAc (2.01 mmol), and catalyst **XI** (1.0 mol %) were combined in a similar procedure as heterocoupling. An analogues workup gave homocoupled products.

[2,2'-Bithiophene]-5,5'-dicarbaldehyde (45a)²⁹: Yellow solid; mp: 190-192 °C; ¹H NMR (400



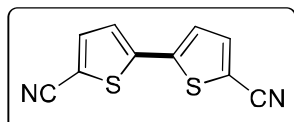
MHz, CDCl₃) δ 9.92 (s, 2H), 7.73 (d, *J* = 4.0 Hz, 2H), 7.43 (d, *J* = 4.0 Hz, 2H); ¹³C{¹H} NMR (100 MHz, CDCl₃) δ 182.6, 144.9, 143.9, 137.0, 126.

1,1'-([2,2'-Bithiophene]-5,5'-diyl)bis(ethan-1-one) (45b)²⁹: Yellow solid; mp: 227-229 °C; ¹H



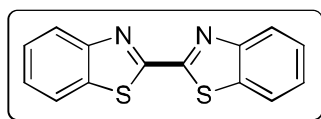
NMR (400 MHz, CDCl₃) δ 7.61 (d, *J* = 4.0 Hz, 2H), 7.30 (d, *J* = 4.0 Hz, 2H), 2.57 (s, 6H); ¹³C{¹H} NMR (100 MHz, CDCl₃) δ 190.4, 144.3, 144.0, 133.2, 126.0, 26.6.

[2,2'-Bithiophene]-5,5'-dicyanitrile (45c): Pale yellow solid; mp: 250-252 °C; ; (Lit.⁸⁸ mp:



252-254 °C); ¹H NMR (400 MHz, CDCl₃) δ 7.59 (d, *J* = 3.9 Hz, 2H), 7.26 (d, *J* = 3.9 Hz, 2H); ¹³C{¹H} NMR (100 MHz, CDCl₃) δ 141.4, 138.3, 125.7, 113.4, 110.2.

2,2'-Bibenzo[*d*]thiazole (45d): White solid; mp; 237-239 °C; (Lit.⁸⁹ mp: 239-240 °C); ¹H NMR



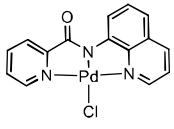
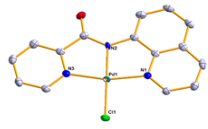
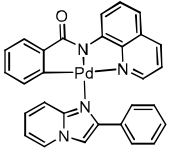
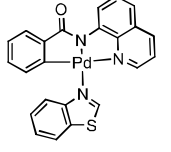
(400 MHz, CDCl₃) δ 8.17 (d, *J* = 8.2 Hz, 2H), 7.99 (d, *J* = 7.9 Hz, 2H), 7.58–7.54 (m, 2H), 7.51–7.47 (m, 2H); ¹³C{¹H} NMR (100 MHz, CDCl₃) δ 161.5, 153.6, 135.8, 126.8, 126.6, 124.1, 122.0.

1.4.9 Procedure for Reusability of Catalyst. In a pressure tube (10 mL) 2-formylthiophene (**9a**, 1.0 mmol), catalyst **XI** (1.0 mol %), AgOAc (2.01 mmol), and DMSO (3 mL) were stirred and heated on 110 °C for 16 h. After 16 h, reaction mixture was cooled to room temperature and small amount of it (150 μL) was used for proton NMR analysis. Thereafter a fresh batch of **9a** and AgOAc was added and reaction was allowed to stir at 110 °C for another 16 h. The analysis of aliquot and addition of fresh substrates was continued for four reaction cycles.

1.4.10 X-ray Crystallographic Analysis of Complexes XI-XIII

A. A CH₃CN (4 mL) solution of **XI** (10 mg) was slowly concentrated over a period of 16 days to afford yellow block like crystals. The data was collected as outlined in **Table 1.3**. Cell parameters were obtained from 45 frames using a 1° scan and refined with 11399 reflections. Integrated intensity information for each reflection was obtained by reduction of the data frames with the program APEX3.⁹⁰ Lorentz and polarization corrections were applied. The absorption correction program SADABS⁹¹ was employed to correct the data for absorption effects. The space group was determined from systematic reflection conditions and statistical tests. The structure was refined (weighted least squares refinement on *F*²) to convergence.⁹²⁻⁹⁴ Olex2⁹⁵ was employed for the final data presentation and structure plots. Non-hydrogen atoms were refined with anisotropic thermal parameters. Hydrogen atoms were fixed in idealized positions using a riding model. The absence of additional symmetry or voids was confirmed using PLATON (ADDSYM).⁹⁶ **B.** A CHCl₃/hexane (4:1) solution of **XII** (10 mg) was slowly concentrated over a period of 13 days to afford colorless block like crystals. The data was collected as outlined in Table s1. The structure was solved as in **A** (45 frames, 26763 reflections). A molecule of chloroform was found solvated. **C.** A CHCl₃/hexane (4:1) solution of **XII** (10 mg) was slowly concentrated over a period of 6 days to afford yellow block like crystals. The data was collected as outlined in **Table 1.3**. The structure was solved as in **A** (45 frames, 9043 reflections). A molecule of chloroform was found solvated. Elongated thermal ellipsoids on (S1, N3, C17-C23), and the solvated chloroform indicated disorder which was modeled successfully between two positions each with an occupancy ratio of 0.51:0.49.

Table 1.3. Crystal data and structure refinement for complex **XI-XII**

| | XI | XII | XIII |
|---|---|---|---|
|  |  |  |  |
| Complex XI | Complex XII | Complex XIII | |
| empirical formula | C ₁₅ H ₁₀ ClN ₃ OPd | C ₃₀ H ₂₁ C ₁₃ N ₄ OPd | C ₂₄ H ₁₆ C ₁₃ N ₃ OPdS |
| formula weight | 390.11 | 666.26 | 607.21 |
| temperature [K] | 110.0 | 110.0 K | 110.0 K |
| diffractometer | Bruker Quest | Bruker Venture | Bruker apex 3 |
| wavelength [Å] | 0.71073 | 1.54178 | 0.71073 |
| crystal system | Monoclinic | Monoclinic | Triclinic |
| space group | <i>P 1 21/c 1</i> | <i>P 1 21/n 1</i> | <i>P-1</i> |
| unit cell dimensions: | | | |
| <i>a</i> [Å] | 17.9412(6) | 9.0855(8) | 10.071(2) |
| <i>b</i> [Å] | 4.5542(10) | 11.3486(10) | 10.666(3) |
| <i>c</i> [Å] | 17.8327(5) | 26.422(2) | 11.180(3) |
| α [°] | 90 | 90 | 76.782(3) |
| β [°] | 114.6150(10) | 92.909(4) | 88.562(3) |
| γ [°] | 90 | 90 | 76.378(3) |
| <i>V</i> [Å ³] | 1324.66(7) | 2720.8(4) | 1135.8(5) |
| <i>Z</i> | 4 | 4 | 2 |
| ρ_{calc} [Mg/m ³] | 1.956 | 1.627 | 1.776 |
| μ [mm ⁻¹] | 1.603 | 8.472 | 1.286 |
| F(000) | 768 | 1336 | 604 |
| crystal size [mm ³] | 0.21 x 0.19 x 0.03 | 0.02 x 0.02 x 0.01 | 0.06 x 0.04 x 0.01 |
| θ limit[°] | 2.706 to 27.496 | 3.350 to 62.377 | 1.872 to 24.718 |
| index range (<i>h, k, l</i>) | -23, 23, -5, 5, -22, 23 | -10, 8, -13, 13, -30, 30 | -11, 11, -12, 12, -13, 13 |
| reflections collected | 11399 | 26763 | 9043 |

| | | | |
|---|-------------------|-------------------|-------------------|
| independent reflections | 3016 | 4302 | 3818 |
| $R(\text{int})$ | 0.0299 | 0.0385 | 0.0572 |
| completeness to θ | 99.6 | 99.6 | 98.6 |
| max. and min. transmission | 0.4330 and 0.3605 | 0.4628 and 0.3091 | 0.4283 and 0.3862 |
| data/restraints/parameters | 3016 / 0 / 190 | 4302 / 36 / 346 | 3818 / 590 / 389 |
| goodness-of-fit on F^2 | 1.093 | 1.140 | 1.011 |
| R indices (final) [$I > 2\sigma(I)$] | | | |
| R_1 | 0.0248 | 0.0329 | 0.0464 |
| wR_1 | 0.0574 | 0.0779 | 0.0892 |
| R indices (all data) | | | |
| R_1 | 0.0303 | 0.0345 | 0.0696 |
| wR_2 | 0.0617 | 0.0788 | 0.0985 |
| largest diff. peak and hole [$\text{e}\text{\AA}^{-3}$] | 0.826 and -0.448 | 1.184 and -0.509 | 0.828 and -0.463 |

1.5. REFERENCES

1. Liu, Y.; Zhang, S.; Abreu, P. J., *Natural Product Reports* **2006**, *23*, 630-651.
2. Hughes, R. A.; Moody, C. J., *Angewandte Chemie* **2007**, *119*, 8076-8101.
3. Corey, E.; Cheng, X., *The Logic of Chemical Synthesis John Wiley & Sons* **1989**.
4. Meijere, A. D.; Diederich, F., *Metal-Catalyzed Cross-Coupling Reactions* **2004**.
5. Bolm, C.; Beller, M., *Transition Metals for Organic Synthesis*. Wiley-VCH: Weinheim: **2004**; Vol. 1.
6. Yamaguchi, J.; Yamaguchi, A. D.; Itami, K., *Angewandte Chemie International Edition* **2012**, *51*, 8960-9009.
7. Miyaura, N.; Buchwald, S. L., *Cross-Coupling Reactions: A Practical Guide*. Springer: **2002**; Vol. 219.
8. Miyaura, N.; Suzuki, A., *Chemical Reviews* **1995**, *95*, 2457-2483.
9. Suzuki, A., *Angewandte Chemie International Edition* **2011**, *50*, 6722-6737.
10. Hapke, M.; Brandt, L.; Lützen, A., *Chemical Society Reviews* **2008**, *37*, 2782-2797.

11. Li, C. J., *Handbook of Green Chemistry; Wiley–VCH: Weinheim, Germany*, Springer: **2012**; Vol. 7.
12. Alberico, D.; Scott, M. E.; Lautens, M., *Chemical Reviews* **2007**, *107*, 174-238.
13. Ackermann, L.; Vicente, R.; Kapdi, A. R., *Angewandte Chemie International Edition* **2009**, *121*, 9976-10011.
14. Gandeepan, P.; Müller, T.; Zell, D.; Cera, G.; Warratz, S.; Ackermann, L., *Chemical Reviews* **2018**, *119*, 2192-2452.
15. Heck, R. F.; Nolley Jr, J., *The Journal of Organic Chemistry* **1972**, *37*, 2320-2322.
16. Corey, E., Cheng, X. M.; *The Logic of Chemical Synthesis*. Wiley, New York: 1989.
17. Yang, Y.; Lan, J.; You, J., *Chemical Reviews* **2017**, *117*, 8787-8863.
18. Yeung, C. S.; Dong, V. M., *Chemical Reviews* **2011**, *111*, 1215-1292.
19. Liu, C.; Yuan, J.; Gao, M.; Tang, S.; Li, W.; Shi, R.; Lei, A., *Chemical Reviews* **2015**, *115*, 12138-12204.
20. Newhouse, T.; Baran, P. S.; Hoffmann, R. W., *Chemical Society Reviews* **2009**, *38*, 3010-3021.
21. Hendrickson, J. B., *Journal of the American Chemical Society* **1975**, *97*, 5784-5800.
22. Segawa, Y.; Maekawa, T.; Itami, K., *Angewandte Chemie International Edition* **2015**, *54*, 66-81.
23. Ackermann, L.; Vicente, R.; Kapdi, A. R., *Angewandte Chemie International Edition* **2009**, *48*, 9792-9826.
24. McGlacken, G. P.; Bateman, L. M., *Chemical Society Reviews* **2009**, *38*, 2447-2464.
25. Dyker, G., *Handbook of C–H Transformations: Applications in Organic Synthesis*. Wiley-VCH: **2005**; Vol. 2.
26. Neufeldt, S. R.; Sanford, M. S., *Accounts of Chemical Research* **2012**, *45*, 936-946.
27. Dong, J.; Huang, Y.; Qin, X.; Cheng, Y.; Hao, J.; Wan, D.; Li, W.; Liu, X.; You, J., *Chemistry—A European Journal* **2012**, *18*, 6158-6162.
28. Cheng, Y.; Li, G.; Liu, Y.; Shi, Y.; Gao, G.; Wu, D.; Lan, J.; You, J., *Journal of the American Chemical Society* **2016**, *138*, 4730-4738.
29. Masui, K.; Ikegami, H.; Mori, A., *Journal of the American Chemical Society* **2004**, *126*, 5074-5075.

30. Takahashi, M.; Masui, K.; Sekiguchi, H.; Kobayashi, N.; Mori, A.; Funahashi, M.; Tamaoki, N., *Journal of the American Chemical Society* **2006**, *128*, 10930-10933.
31. Xia, J. B.; Wang, X. Q.; You, S. L., *The Journal of Organic Chemistry* **2009**, *74*, 456-458.
32. Xi, P.; Yang, F.; Qin, S.; Zhao, D.; Lan, J.; Gao, G.; Hu, C.; You, J., *Journal of the American Chemical Society* **2010**, *132*, 1822-1824.
33. Han, W.; Mayer, P.; Ofial, A. R., *Angewandte Chemie International Edition* **2011**, *50*, 2178-2182.
34. Chen, X.; Huang, X.; He, Q.; Xie, Y.; Yang, C., *Chemical Communications* **2014**, *50*, 3996-3999.
35. Guo, T.; Liang, J. J.; Yang, S.; Chen, H.; Fu, Y. N.; Han, S. L.; Zhao, Y. H., *Organic & Biomolecular Chemistry* **2018**, *16*, 6039-6046.
36. Sau, S. C.; Vardhanapu, P. K.; Mandal, S. K., *The Journal of Organic Chemistry* **2018**, *83*, 9403-9411.
37. Tsuji, J., *Palladium Reagents and Catalysts: New Perspectives for the 21st Century*. **2006**.
38. Biffis, A.; Centomo, P.; Del Zotto, A.; Zecca, M., *Chemical Reviews* **2018**, *118*, 2249-2295.
39. Muniz, K., *Angewandte Chemie International Edition* **2009**, *48*, 9412-9423.
40. Hartwig, J. F., *Organotransition Metal Chemistry: From Bonding to Catalysis*. University Science Books: **2010**.
41. Moulton, C. J.; Shaw, B. L., *Journal of the Chemical Society, Dalton Transactions* **1976**, 1020-1024.
42. Van Koten, G.; Timmer, K.; Noltes, J. G.; Spek, A. L., *Journal of the Chemical Society, Chemical Communications* **1978**, 250-252.
43. Van Der Boom, M. E.; Milstein, D., *Chemical Reviews* **2003**, *103*, 1759-1792.
44. Herrmann, W. A.; Böhm, V. P.; Reisinger, C.-P., *Journal of Organometallic Chemistry* **1999**, *576*, 23-41.
45. Beletskaya, I. P.; Cheprakov, A. V., *Journal of Organometallic Chemistry* **2004**, *689*, 4055-4082.
46. Dupont, J.; Pfeffer, M., *Palladacycles: Synthesis, Characterization and Applications*. John Wiley & Sons: **2008**.

47. Cope, A. C.; Friedrich, E. C., *Journal of the American Chemical Society* **1968**, *90*, 909-913.
48. Frutos-Pedreno, R.; Garcia-Sanchez, E.; Oliva-Madrid, M. J.; Bautista, D.; Martinez-Viviente, E.; Saura-Llamas, I.; Vicente, J., *Inorganic Chemistry* **2016**, *55*, 5520-5533.
49. Dehand, J.; Pfeffer, M.; Zinsius, M., *Inorganica Chimica Acta* **1975**, *13*, 229-232.
50. Braunstein, P.; Dehand, J.; Pfeffer, M., *Inorganic and Nuclear Chemistry Letters* **1974**, *10*, 581-585.
51. Morales-Morales, D.; Redón, R.; Yung, C.; Jensen, C. M., *Chemical Communications* **2000**, 1619-1620.
52. Valk, J. M.; Boersma, J.; Van Koten, G., *Journal of Organometallic Chemistry* **1994**, *483*, 213-216.
53. Trofimenko, S., *Inorganic Chemistry* **1973**, *12*, 1215-1221.
54. Consorti, C. S.; Ebeling, G.; Flores, F. R.; Rominger, F.; Dupont, J., *Advanced Synthesis & Catalysis* **2004**, *346*, 617-624.
55. Yang, M. J.; Liu, Y. J.; Gong, J. F.; Song, M. P., *Organometallics* **2011**, *30*, 3793-3803.
56. Hou, A. T.; Liu, Y. J.; Hao, X. Q.; Gong, J. F.; Song, M. P., *Journal of Organometallic Chemistry* **2011**, *696*, 2857-2862.
57. McPherson, H. M.; Wardell, J. L., *Inorganica Chimica Acta* **1983**, *75*, 37-43.
58. Solé, D.; Vallverdú, L.; Solans, X.; Font-Bardía, M.; Bonjoch, J., *Journal of the American Chemical Society* **2003**, *125*, 1587-1594.
59. Zim, D.; Buchwald, S. L., *Organic Letters* **2003**, *5*, 2413-2415.
60. Dijkstra, H. P.; Slagt, M. Q.; McDonald, A.; Kruithof, C. A.; Kreiter, R.; Mills, A. M.; Lutz, M.; Spek, A. L.; Klopffer, W.; Klink, G. P. V., *European Journal of Inorganic Chemistry* **2003**, *2003*, 830-838.
61. Selander, N.; Szabó, K. J., *Chemical Reviews* **2011**, *111*, 2048-2076.
62. Jung, I. G.; Son, S. U.; Park, K. H.; Chung, K. C.; Lee, J. W.; Chung, Y. K., *Organometallics* **2003**, *22*, 4715-4720.
63. Takenaka, K.; Uozumi, Y., *Organic Letters* **2004**, *6*, 1833-1835.
64. Takemoto, T.; Iwasa, S.; Hamada, H.; Shibatomi, K.; Kameyama, M.; Motoyama, Y.; Nishiyama, H., *Tetrahedron Letters* **2007**, *48*, 3397-3401.
65. Bugarin, A.; Connell, B. T., *Chemical Communications* **2011**, *47*, 7218-7220.

66. Luo, Q. L.; Tan, J. P.; Li, Z. F.; Qin, Y.; Ma, L.; Xiao, D. R., *Dalton Transactions* **2011**, 40, 3601-3609.
67. Wang, T.; Hao, X. Q.; Zhang, X. X.; Gong, J. F.; Song, M. P., *Dalton Transactions* **2011**, 40, 8964-8976.
68. Zhang, J. H.; Li, P.; Hu, W. P.; Wang, H. X., *Polyhedron* **2015**, 96, 107-112.
69. Yadav, S.; Dash, C., *Tetrahedron* **2020**, 76, 131-135.
70. Kiani, M.; Bagherzadeh, M.; Meghdadi, S.; Fadaei-Tirani, F.; Schenk-Joß, K.; Rabiee, N., *Applied Organometallic Chemistry* **2020**, 34, e5531.
71. Yu, X.; Yang, F.; Wu, Y.; Wu, Y., *Organic Letters* **2019**, 21, 1726-1729.
72. Zhang, S.-Y.; Li, Q.; He, G.; Nack, W. A.; Chen, G., *Journal of the American Chemical Society* **2015**, 137, 531-539.
73. He, Q.; Ano, Y.; Chatani, N., *Chemical Communications* **2019**, 55, 9983-9986.
74. Meng, Y. Y.; Si, X. J.; Song, Y. Y.; Zhou, H. M.; Xu, F., *Chemical Communications* **2019**, 55, 9507-9510.
75. Bhaskar, R.; Sharma, A. K.; Singh, A. K., *Organometallics* **2018**, 37, 2669-2681.
76. Sharma, K. N.; Joshi, H.; Singh, V. V.; Singh, P.; Singh, A. K., *Dalton Transactions* **2013**, 42, 3908-3918.
77. Joshi, H.; Prakash, O.; Sharma, A. K.; Sharma, K. N.; Singh, A. K., *European Journal of Inorganic Chemistry* **2015**, 2015, 1542-1551.
78. Liang, Z.; Zhao, J.; Zhang, Y., *The Journal of Organic Chemistry* **2009**, 75, 170-177.
79. Shi, Y.; Wang, Z.; Cheng, Y.; Lan, J.; She, Z.; You, J., *Science China Chemistry* **2015**, 58, 1292-1296.
80. Arockiam, P. B.; Guillemard, L.; Wencel-Delord, J., *Advanced Synthesis & Catalysis* **2017**, 359, 2571-2579.
81. Li, Q.; Zhou, M.; Han, L.; Cao, Q.; Wang, X.; Zhao, L.; Zhou, J.; Zhang, H., *Chemical Biology & Drug Design* **2015**, 86, 849-856.
82. Meghdadi, S.; Amirnasr, M.; Amiri, A.; Mobarakeh, Z. M.; Azarkamanzad, Z., *Comptes Rendus Chimie* **2014**, 17, 477-483.
83. Su, H.; Wang, L.; Rao, H.; Xu, H., *Organic Letters* **2017**, 19, 2226-2229.
84. Xi, P.; Yang, F.; Qin, S.; Zhao, D.; Lan, J.; Gao, G.; Hu, C.; You, J., *Journal of the American Chemical Society* **2010**, 132, 1822-1824.

85. P, S.; Sau, S. C.; Vardhanapu, P. K.; Mandal, S. K., *The Journal of Organic Chemistry* **2018**, *83*, 9403-9411.
86. El'chaninov, M.; Simonov, A.; Simkin, B. Y., *Chemistry of Heterocyclic Compounds* **1982**, *18*, 833-835.
87. Qin, X.; Feng, B.; Dong, J.; Li, X.; Xue, Y.; Lan, J.; You, J., *The Journal of Organic Chemistry* **2012**, *77*, 7677-7683.
88. MacKinnon, C. D.; Parent, S. L.; Mawhinney, R. C.; Assoud, A.; Robertson, C. M., *CrystEngComm* **2009**, *11*, 160-167.
89. Zhu, M.; Fujita, K. I.; Yamaguchi, R., *Chemical Communications* **2011**, *47*, 12876-12878.
90. APEX3, *Bruker AXS Inc., Madison, WI, USA*, **2012**.
91. Sheldrick, G. M. S., *Bruker AXS Inc., Madison, WI, USA*, **2001**.
92. Sheldrick, G. M. S., *Acta Crystallographica* **2008**, *A64*, 112-122.
93. Sheldrick, G. M., *Acta Crystallographica* **2015**, *A71*, 3-8.
94. Sheldrick, G. M., *Acta Crystallographica* **2015**, *C71*, 3-8.
95. Dolomanov, O. V.; Bourhis, L. J.; Gildea, R. J.; Howard, J. A.; Puschmann, H., *Journal of Applied Crystallography* **2009**, *42*, 339-341.
96. Spek, A. L., *Journal of Applied Crystallography* **2003**, *36*, 7-13.